ARPA ORDER NO.: 189-1
7G10 Tactical Technology

R-2111-ARPA
June 1977

Entry Flow in a Heated Tube

Lun-Shin Yao

A Report prepared for

DEFENSE ADVANCED RESEARCH PROJECTS AGENCY

Rand
SANTA MONICA, CA. 90406

The research described in this report was sponsored by the Defense Advanced Research Projects Agency under Contract No. DAHC15-73-C-0181.

Published by The Rand Corporation

PREFACE

Under the sponsorship of the Tactical Technology Office of the Defense Advanced Research Projects Agency, The Rand Corporation has been engaged in the analysis and development of hydrodynamic design criteria employing concepts of boundary-layer control, including shaping, suction, and heating.

This report supplies a theoretical explanation of flow development in a heated pipe. The analysis shows that a secondary flow is generated in the core of the pipe by heating the wall, and that this flow differs from that over the exterior of bodies of revolution. The results define domains where this secondary flow can be neglected and where test data can be used in interpreting exterior flow. They are applied to a tube test set up at Colorado State University, Fort Collins, Colorado, by the Autonetics Division of Rockwell International, to experimentally verify theories predicting stabilization of the boundary layer by heating, shaping, and other means.

This report should be useful to hydrodynamicists, to designers of submersibles, and to others interested in applying fluid mechanics to improve the performance of underwater vehicles.

Other related Rand publications include:

R-1752-ARPA/ONR, *Low-Speed Boundary-Layer Transition Workshop*, W. S. King, June 1975.

R-1789-ARPA, *Controlling the Separation of Laminar Boundary Layers in Water: Heating and Suction*, J. Aroesty and S. A. Berger, September 1975.

R-1863-ARPA, *The Effects of Wall Temperature and Suction on Laminar Boundary-Layer Stability*, W. S. King, April 1976.

R-1898-ARPA, *"e^9": Stability Theory and Boundary-Layer Transition*, S. A. Berger and J. Aroesty, February 1977.

R-1907-ARPA, *Buoyancy Cross-Flow Effects on the Boundary Layer of a Heated Horizontal Cylinder*, L. S. Yao and I. Catton, April 1976.

R-1966-ARPA, *The Buoyancy and Variable Viscosity Effects on a Water Laminar Boundary Layer Along a Heated Longitudinal Horizontal Cylinder*, L. S. Yao and I. Catton, February 1977.

SUMMARY

The developing flow in the entry region of a heated horizontal pipe is analyzed. Due to the similarity of flow phenomena between heated straight pipes and unheated curved pipes, the techniques developed in treating the flow problem in the latter can be applied to study the flow development in the former. The asymptotic solution of the developing flow near the entrance of the heated straight pipe, distance $O(a)$, is obtained by perturbing the solution of the developing flow in an unheated straight pipe. Two vortices result from the combination of the radial-directional and the downward motions of the fluid particles which are induced by the displacement of the boundary layer and develop along the pipe. The axial velocity has a concave profile with its maximum off the center line near the entrance, and it grows toward a uniformly distributed profile downstream. The downward stream caused by the displacement of the secondary boundary layer forces the axial velocity profile to turn counterclockwise continuously along the pipe if the flow is from left to right. A favorable pressure gradient is generated on the bottom wall of the pipe; an unfavorable pressure gradient is induced on the top wall.

The results of the analysis are applied to the "Colorado tube test" set. It has been found that under test conditions, when the flow speed is not fast enough, strong wall heating can cause the boundary-layer flow to separate from the top wall of the pipe, causing transition to turbulence; in this case the pipe flow cannot be used to simulate an external boundary-layer flow.

ACKNOWLEDGMENTS

Special thanks are due Mario Juncosa of Rand for the suggestion of applying Fast Fourier Transform in the numerical integration of Eqs. (27a,b) and (30a), for help in deriving the methods, and for stimulating discussions.

CONTENTS

SYMBOLS

a = radius of the pipe

A = variable viscosity function, Eq. (13)

D = Dean number, $= \alpha^{-\frac{1}{2}} \cdot Re$

f_0, F_1, F_2 = dimensionless stream functions

g = gravitational acceleration = 32.2 ft/sec^2

G = dimensionless temperature function

Gr = Grashof number $= \dfrac{\gamma g a^3 \Delta T}{\nu^2}$

I_0, I_1, I_2 = Bessel functions

k = thermal conductivity

N_0, N = viscosity ratio, Eq. (13)

P = pressure

Pr = Prandtl number

q_w = wall heat flux, Eq. (1)

r, ϕ, z = coordinates, Fig. 1 (ft)

$\bar{r}$ = coordinate normal to the wall

Ra = Rayleigh number

Re = Reynolds number

T = temperature (°F)

$\Delta T = T_w - T_{in}$ (°F)

T_w = wall temperature (°F)

T_{in} = inlet temperature (°F)

u, v, w = velocities in the boundary layer (ft/sec)

U, V, W = velocities of the inviscid core flow (ft/sec)

X, Y, z = coordinates, Fig. 1

$\bar{\alpha}$ = curvature ratio

α = constant viscosity, Eq. (13)

β_1, β_2, β_3 = constants, Table 1

γ = expansion coefficient

$\delta = \dfrac{1}{\sqrt{Re}}$

$\varepsilon = \dfrac{Gr}{Re^2}$, Eq. (7)

η = Blasius variable

θ_0, Θ = dimensionless temperature $= \begin{cases} \dfrac{T - T_{in}}{T_w - T_{in}} & \text{(constant } T_w\text{)} \\ \dfrac{T - T_{in}}{\dfrac{a\, q_w}{k\sqrt{Re}}} & \text{(constant } q_w\text{)} \end{cases}$

Θ_c = dimensionless temperature at r = 0

κ = thermal diffusivity

ν = kinematic viscosity, Eq. (1)

Subscripts

0, 01, 10, 11 indicate the order of the perturbing functions

I. INTRODUCTION

The laminar flow convective heat transfer in a pipe has been a research topic for about half a century. Continuous efforts have been devoted to the topic due to its practical applications in various engineering systems. It has been found that natural convection and variable material properties play important roles in the heat transfer and the fluid flow in a heated pipe. Frequently the prediction of the heat transfer by forced convection alone, without considering the secondary flow, can cause large errors. Comprehensive reviews of previous work can be found in two recent papers by Siegwarth et al. (1969) and Hong and Bergles (1976). Of the early works, three papers worthy of special attention are summarized below.

Morton (1959) found that the flow in a heated straight pipe is similar to that in a curved pipe. He followed the similar expansion technique developed by Dean (1927, 1928) in solving the problem of a fully developed flow in curved pipes and was able to give the solution of laminar convection in uniformly heated horizontal pipes. He showed that the expansion parameter is the Rayleigh number, Ra (or the Grashof number, Gr). However, for a constant wall heat flux condition, the heat transfer is enhanced by the speed of the flow and the length of a heated pipe. Therefore, the flow velocities and the heat transfer also depend on the Reynolds number, Re. Consequently, the solutions of constant wall heat flux depends on the product of the Rayleigh and the Reynolds numbers, RaRe. Since the analysis given by Dean is limited to the case of small Dean number, D, the ratio of the centrifugal force and the viscous force, the Morton solution is also valid only when ReRa, the ratio of the buoyancy force and the viscous force, is small in a heated pipe. For the curved pipe flow of large D, Baura (1963) observed that viscous forces are important only in a thin boundary layer near the wall and that the motion outside the boundary layer is mostly confined to planes parallel to the plane of symmetry of the pipe. With these observations and assumptions, Baura obtained an asymptotic boundary-layer solution; the resistance coefficient obtained from this

theory agrees with the observations of White and Adler (see Baura, 1963). Mori and Futagami (1967) presented a theoretical model similar to Baura's ideal; the Nusselt number obtained from their model agrees well with their experimental data. Another interesting character of the flow in heated pipes, revealed by Mori et al. (1965) is that the secondary flow generated by heating can suppress the turbulence level when the inlet turbulence level is high and can enhance it when its level is low at the inlet. They also found that the critical Reynolds number of the flow in heated pipes converges to a value approximately equal to 3.8×10^3 at $\mathrm{ReRa} = 5 \times 10^5$ independently on the inlet turbulence level. The similar phenomenon was observed by Taylor (1929) for the flow in curved pipes.

In this report we study the entry-developing flow in a heated straight pipe under the conditions of constant wall temperature and constant wall heat flux, respectively. The inlet velocity, W_{in}, is uniformly distributed. The wall of the pipe is maintained either at a higher temperature, T_w, than the inlet fluid temperature, T_{in}, or at the constant heat flux, q_w. The governing parameters of the problem are (see Eqs. (2) in Section II):

$$\left.\begin{aligned}
&\text{(i)}\quad \text{the Reynolds number} \quad \mathrm{Re} = \frac{W_{in}a}{\nu} \\
&\text{(ii)}\quad \text{the Grashof number} \quad \mathrm{Gr} = \frac{\gamma g a^3 (T_w - T_{in})}{\nu^2} \quad \text{(constant wall temperature)} \\
&\qquad\qquad\qquad\qquad = \frac{\gamma g a^4 q_w}{k\nu^2} \quad \text{(constant wall heat flux)} \\
&\text{(iii)}\quad \text{the Prandtl number} \quad \mathrm{Pr} = \frac{\nu}{\kappa} \\
&\text{(iv)}\quad \text{the ratio} \quad \varepsilon = \frac{\mathrm{Gr}}{\mathrm{Re}^2} \quad \text{(constant wall temperature)} \\
&\qquad\qquad\qquad\qquad = \frac{\mathrm{Gr}}{\mathrm{Re}^{5/2}} \quad \text{(constant wall heat flux)}
\end{aligned}\right\} \quad (1)$$

where a is the radius of the pipe, ν is the kinematic viscosity, β is the thermal expansion coefficient, g is the gravitational acceleration, and κ is the thermal diffusivity.

Since the development of the entry flow in heated pipes is similar to that of curved pipes and the solution we will present is obtained by perturbing the entry flow in unheated straight pipes, we shall briefly review previous work on the entry flow in unheated straight pipes and curved pipes.

UNHEATED STRAIGHT PIPES

Previous work on developing flow in unheated straight pipes and two-dimensional channels falls into the following four categories: (i) linearization of the momentum equations; (ii) two-zone models, in which a boundary-layer flow matches with the downstream perturbation solution for the fully developed flow; (iii) momentum-integral techniques; and (iv) finite-difference solutions. A detailed review of the published papers falling into the above four categories has been summarized by Yao and Berger (1975). From a critical analysis of the entry flow problem, Van Dyke (1970) pointed out that there are two length scales in channel entry flow: a, the half-width of the channel, and aRe. Most of the early work on this problem is valid only for downstream distance O(aRe). Van Dyke obtained a solution in the upstream region, for distance O(a), and so reconciled the discrepancy between the earlier theoretical results and the experimental data near the entrance of the channel. Independently, a similar but more detailed mathematical analysis was given by Wilson (1971).

CURVED PIPE

Two parameters govern the developing entry flow in curved pipes: $\bar{\alpha}$, the curvature ratio, and $D = \bar{\alpha}^{1/2}Re$, the Dean number. The entry flow in curved pipes can be categorized into the following three cases:

1. When both α and D are small, the flow is slightly distorted from the entry flow in unheated straight pipes, and the solution can be obtained by perturbing the solution of the developing flow in unheated straight pipes. There are two regions: O(a) and O(aRe). The solution in the region, for distance O(a), was given by Singh (1974). As the fluid enters the pipe, a boundary layer like that in an unheated straight

pipe develops on the wall but with a small azimuthal component of velocity due to the inwardly directed pressure gradient, the latter arising from the circular nature of the main central flow. The displacement effect of the boundary layer in turn causes an acceleration of the flow in the central core plus a secondary flow in the cross-sectional plane. Initially there is an inward flow from the entire pipe circumference, with two singularities in the central region, a node-like sink at the origin, and a saddle-point-like stagnation point; the latter singularity moves outwards as the fluid moves downstream, finally vanishing as the cross flow (from the inside to the outside of the bend) sets in. (For further details, plus the interesting consequences this flow picture has on the location of the point of maximum shear, see Singh (1974).) The flow development described above occurs within a distance 0(a) from the entrance. The matched asymptotic solution for this region (Singh, 1974) breaks down at a distance $0(a/\sqrt{\bar{\alpha}})$, corresponding physically to the point beyond which the effect of the centrifugal force, initially small, becomes as important as inertia and viscous forces within the boundary layer. Also, the matched asymptotic solution developed for the region, distance 0(a), apparently breaks down at a distance 0(aRe), since aRe is the length scale of the region that flow transits to the fully developed flow in unheated straight pipes. There are two possible length scales for the region downstream of the region distance 0(a) from the entrance. However, $aRe < a/\sqrt{\bar{\alpha}}$ when D is small. This suggests that the flow will be fully developed before centrifugal forces lose their secondary role, when D is small.

2. For the case when $\bar{\alpha}$ is small and D is large, the flow appears to develop as follows. At the very beginning, in the region of 0(a), the flow develops as described above. However, the centrifugal force becomes one of the dominant forces as the fluid moves into the next region, a distance of $0(a/\sqrt{\bar{\alpha}})$. Much of the flow development occurs within a distance of $0(a/\sqrt{\bar{\alpha}})$. The variation of the centrifugal force and the pressure gradient directed away from the center of curvature on a cross section of the pipe is small, since α is generally smaller than one for most curved pipes of interest. The resultant of the nearly

uniformly distributed pressure gradient and the strong centrifugal force will accelerate the fluid in the central core. The flow is nealy uniform from the inner to the outer wall of the tube (away from the center of curvature). The boundary layer acts as a reservoir, receiving the fluid moving towards the outer wall, and also as a source of fluid leaving it at the inner wall. The resulting cross flow forms a stagnation-like flow locally along the outer wall of the pipe. The convective effect of this locally stagnant flow prevents the secondary boundary layer from growing. Thus, the secondary boundary layer will remain thin as the flow asymptotically approaches the fully developed state (Baura's flow) in the region of distance $0(aRe/\sqrt{D})$. There are three length scales: a, $a/\sqrt{\bar{\alpha}}$, $aRe/\sqrt{D}$ for this case. The solutions of regions, distances $0(a/\sqrt{\bar{\alpha}})$ and $0(aRe/\sqrt{D})$ were given by Yao and Berger (1975). It is interesting to note that the size of the region where Singh's flow is valid depends on the values of α. It shrinks as the values of α increase.

3. When both $\bar{\alpha}$ and D are large, the region governed by Singh's flow is shrunk to zero. (It should be noted that when we say that $\bar{\alpha}$ is large it does not imply that the value of $\bar{\alpha}$ is larger than one. It simply means that the value of $\bar{\alpha}$ is not close to zero.) For this case, the developing flow is governed by the solution presented by Yao and Berger (1975).

HEATED STRAIGHT PIPE

The developing flow in heated straight pipes can be categorized into cases similar to the developing flow in curved pipes. It should be noted that the fully developed flow in heated straight pipes under the condition of constant wall temperature is simply the Poiseuille flow, and the ones under the condition of constant wall heat flux are given by Morton (1958) if ReRa is small and by Mori and Futagami (1967) if ReRa is large. Three categories of the developing flows are:

(i) When ε and Gr are small, the entry flow deviates slightly from the developing Poiseuille flow. There are two

regions: $0(a)$ and $0(aRe)$, which are similar to the entry flow in an unheated pipe.

(ii) When ε is small and Gr is large, the axial-length scales are $0(a)$ and $0(aRe^{4/5}/Gr^{2/5})$ for the constant wall heat flux and $0(a)$, $0(aRe/Gr^{1/2})$ and $0(aRe)$ for constant wall temperature. The secondary flow becomes one of the dominant flow components as the fluid moves into the region of $0(aRe/Gr^{1/2})$ for constant wall temperature). For constant heat flux, the flow approaches its fully developed state at the end of region $0(aRe^{4/5}/Gr^{2/5})$. For the case of constant wall temperature, the temperature difference between the wall and the core flow decreases in the region of $0(aRe)$, and the flow approaches its fully-developed state, Poiseuille flow.

(iii) When ε is large, the region of $0(a)$ does not exist. The rest of the flow development is similar to case (ii).

The solution presented in this report is limited to the region distance $0(a)^*$ from the inlet for both constant wall temperature and wall heat flux conditions The solution exists, apparently, when ε is small.

As the fluid enters the pipe, a boundary layer develops on the wall with a secondary flow developed inside the boundary layer by the buoyancy forces due to the temperature difference between the wall and the inlet fluid. The central inviscid flow will be accelerated by the displacement of the axial boundary layer like that in an unheated straight pipe. This motion generates node-like sinks along the center line of the pipe and causes fluid particles to move toward the center of the pipe. Simultaneously, the displacement of the secondary boundary layer induces a uniform, downward stream on the cross-section of the pipe. The combination of the downward stream with the radial stream responds to the development of two vortices in the central core of the pipe. A saddle-point-like stagnation point, initially coincident with the center line, moves downward along the vertical symmetry

---

*The solution in the region of $0(a)$ has been proved to be valid when $z \leq 0.46/\sqrt{\varepsilon}$ for external flow.

line of the pipe, and the saddle-point-like stagnation point will stay in the core of the pipe within the region of $0(a)$. The axial velocity profile turns counterclockwise to accommodate the downward stream generated by the displacement of the secondary boundary layer. A favorable pressure gradient develops along the bottom wall of the pipe; on the contrary, an unfavorable pressure gradient develops along the top wall of the pipe. It is found that the temperature in the central core of the pipe does not change within the region of $0(a)$ and is identical to the inlet temperature. It is expected that the strength of the sinks along the pipe center line will gradually decrease and the downward-stream pattern will become dominant as the fluid moves downstream of the region, a distance $0(a)$ from the inlet when Gr is large.

The theory developed above has been applied to the "Colorado tube test." The range that heating stabilizes the boundary layer can be found in the region, a distance $0(a)$ from the inlet, and the secondary flow will be negligible in this region since the values of ε for the tests are very small. Downstream of the region of $0(a)$, the unfavorable pressure gradient along the top wall of the pipe can force the flow to separate. The test would be successful if the flow in the test section can be restricted to the region distance $0(a)$ from the inlet. The size of this region shrinks when the value of ε increases. A detailed evaluation of the possible test range of the laminar flow is given in Section V.

II. GOVERNING EQUATIONS

Near the inlet it is natural to refer lengths to the radius a of the pipe, and velocities to the uniform inlet velocity, W_{in} (Fig. 1). The pressure is nondimensionalized by $\rho_{in} W_{in}^2$, where ρ_{in} is the density. The dimensionless temperature is defined in terms of the inlet temperature, T_{in}, and the constant wall temperature, T_w, as $\Theta = (T - T_{in})/(T_w - T_{in})$, or the constant wall heat flux, q_w, as $\Theta = (T - T_{in})\, k\sqrt{Re}/a \cdot q_w$. The dimensionless equations of motion and energy with the Boussinesq approximation in cylindrical coordinates become

$$\frac{1}{r}\frac{\partial (rU)}{\partial r} + \frac{1}{r}\frac{\partial V}{\partial \phi} + \frac{\partial W}{\partial z} = 0 \tag{2a}$$

$$U\frac{\partial U}{\partial r} + \frac{V}{r}\frac{\partial U}{\partial \phi} + W\frac{\partial U}{\partial z} - \frac{V^2}{r} = -\frac{\partial P}{\partial r} + \varepsilon(\Theta - \Theta_c)\cos\phi + \frac{1}{Re}\left(\nabla^2 U - \frac{U}{r^2} - \frac{2}{r^2}\frac{\partial V}{\partial \phi}\right) \tag{2b}$$

$$U\frac{\partial V}{\partial r} + \frac{V}{r}\frac{\partial V}{\partial \phi} + W\frac{\partial V}{\partial z} + \frac{UV}{r} = -\frac{\partial P}{r\partial \phi} + \varepsilon(\Theta - \Theta_c)\sin\phi + \frac{1}{Re}\left(\nabla^2 V - \frac{V}{r^2} + \frac{2}{r^2}\frac{\partial U}{\partial \phi}\right) \tag{2c}$$

$$U\frac{\partial W}{\partial r} + \frac{V}{r}\frac{\partial W}{\partial \phi} + W\frac{\partial W}{\partial z} = -\frac{\partial P}{\partial z} + \frac{1}{Re}\nabla^2 W \tag{2d}$$

$$U\frac{\partial \Theta}{\partial r} + \frac{V}{r}\frac{\partial \Theta}{\partial \phi} + W\frac{\partial \Theta}{\partial z} = \frac{1}{Pr\ Re}\nabla^2 \Theta \tag{2e}$$

where

$$\nabla^2 = \frac{\partial^2}{\partial r^2} + \frac{1}{r}\frac{\partial}{\partial r} + \frac{1}{r^2}\frac{\partial^2}{\partial \phi^2} + \frac{\partial^2}{\partial z^2} \tag{3}$$

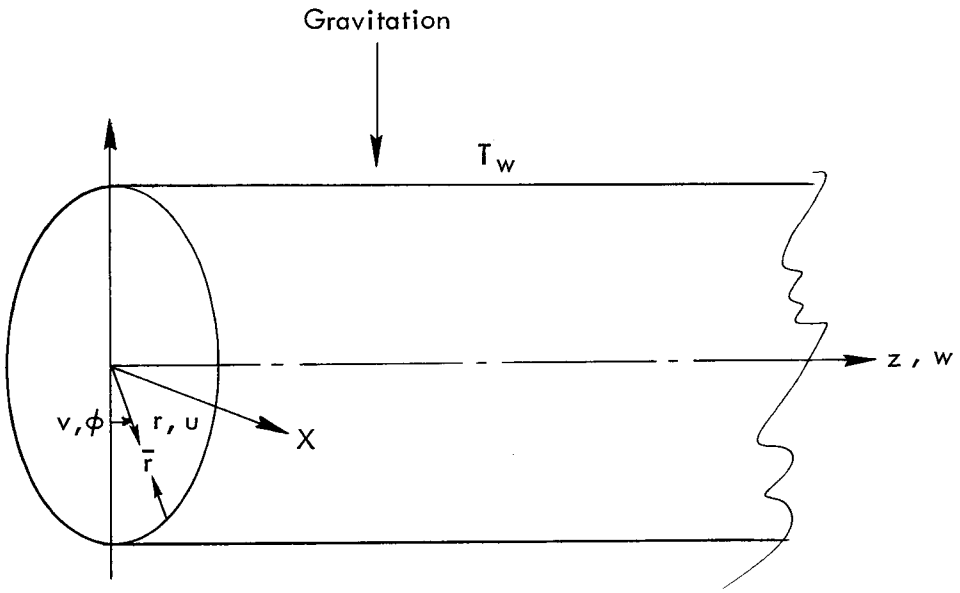

Fig. 1 — Coordinate systems

is the Laplace operator and Θ_c is the temperature along the center line of the pipe. The parameters ε, Re and Pr are defined in Eq. (1).

The entry condition is uniform inlet axial velocity and temperature; the reference pressure at the inlet is set equal to zero. It may be noted that, in the absence of viscosity, the exact solution of Eqs. (2) satisfying the above inlet condition and slip wall condition is

$$W = 1, \qquad U = V = P = \Theta = 0 \tag{4}$$

III. SOLUTIONS

As the fluid flows into the pipe, the viscous forces are confined to the thin boundary layer near the wall of the pipe. For a heated pipe the secondary flow is created by the buoyancy forces inside the thermal boundary layer. The ratio of the thicknesses of the thermal boundary layer to the momentum boundary layer depends on the Prandtl number. Viscous forces and heat conduction away from the boundary layer can be ignored; the flow is isothermal and inviscid in the central core of the pipe. The core flow is accelerated due to the displacement effect of the boundary layer and fluid particles will be pushed from the wall toward the center of the pipe. Simultaneously, a downward stream is developed due to the displacement effect of the secondary boundary layer. The combination of the radial-direction motion with the downward one gives the stream pattern of two developing vortices on the cross-section normal to the axis of the pipe. The downward stream will also skew the axial velocity by accelerating it below the center and decelerating it above the center of the pipe. The analysis shows that the development of the secondary flow due to the heating effect near the entrance when ε is small can be obtained by perturbing the solution of the developing flow in an unheated pipe.

ZEROTH-ORDER SOLUTION IN THE INVISCID CORE

The solution of the inviscid core flow can be obtained by expanding the dependent variables into series in δ which are

$$\left.\begin{aligned} U &= U_0 + \delta U_1 + \dots \\ V &= V_0 + \delta V_1 + \dots \\ W &= W_0 + \delta W_1 + \dots \\ P &= P_0 + \delta P_1 + \dots \\ \Theta &= \Theta_0 + \delta \Theta_1 + \dots \\ \Theta_c &= \Theta_0^c + \delta \Theta_1^c + \dots \end{aligned}\right\} \qquad (5)$$

where δ, the expansion parameter, can be determined by matching with the zeroth order boundary-layer flow. It can be shown that it is equal to $1/\sqrt{Re}$. The governing equations of the first order can be obtained by taking the limit of $Re \to \infty$ from Eqs. (2). The zeroth solutions which satisfy the uniform inlet velocity and temperature conditions and the slip condition at the pipe wall are the undisturbed flow, which is given in Eq. (4).

ZEROTH-ORDER BOUNDARY-LAYER FLOW

Near the pipe wall, the viscous forces and heat conduction normal to the wall become important. The radial coordinate r is stretched to reflect this physical fact. Accordingly, we introduce the inner variables, as in the classical boundary layer,

$$r = 1 - \delta\bar{r}, \qquad U = -\delta u, \qquad V(r,\phi,z) = v(\bar{r},\phi,z), \text{ etc.} \tag{6}$$

A combination of Eqs. (2) and (6), after neglecting the smaller order terms, yields

$$\left.\begin{aligned} \frac{\partial u}{\partial \bar{r}} + \frac{\partial v}{\partial \phi} + \frac{\partial w}{\partial z} &= 0 \\ u\frac{\partial v}{\partial \bar{r}} + v\frac{\partial v}{\partial \phi} + w\frac{\partial v}{\partial z} &= -\frac{\partial P}{\partial \phi} + \varepsilon(\theta - \theta_c)\sin\phi + \frac{\partial^2 v}{\partial \bar{r}^2} \\ u\frac{\partial w}{\partial \bar{r}} + v\frac{\partial w}{\partial \phi} + w\frac{\partial w}{\partial z} &= -\frac{\partial P}{\partial z} + \frac{\partial^2 w}{\partial \bar{r}^2} \\ u\frac{\partial \theta}{\partial \bar{r}} + v\frac{\partial \theta}{\partial \phi} + w\frac{\partial \theta}{\partial z} &= \frac{1}{Pr}\frac{\partial^2 \theta}{\partial \bar{r}^2} \end{aligned}\right\} \tag{7}$$

The analysis of the first-order boundary-layer flow can be easily extended to the case in which fluid properties depend on the temperature. For most liquids, the principal departure from constant-property flow is due to the viscosity variation. Including the variable viscosity of the fluid, the terms of the viscous forces in Eqs. (7) will be replaced by

$$\frac{\partial^2 v}{\partial \bar{r}^2} \to \frac{\partial}{\partial \bar{r}}\left(N \frac{\partial v}{\partial \bar{r}}\right)$$

$$\frac{\partial^2 w}{\partial \bar{r}^2} \to \frac{\partial}{\partial \bar{r}}\left(N \frac{\partial w}{\partial \bar{r}}\right) \tag{8}$$

where

$$N = \frac{\mu}{\mu_\infty}$$

is the viscosity normalized by the viscosity in the central core. The associated boundary conditions of Eqs. (7) are

$$\left.\begin{array}{ll}
\text{At } z = 0,\ u = v = \theta = 0,\ w = 1 & \text{(entrance condition)} \\
\text{At } \bar{r} = 0,\ u = v = w = 0, & \text{(no-slip condition at wall)} \\
\qquad \theta = 1, \text{ or} & \text{(constant wall temperature)} \\
\qquad \theta_{\bar{r}} = -1 & \text{(constant wall heat flux)} \\
\text{As } \bar{r} \to \infty,\ v \to 0,\ w \to 1,\ \theta \to 0 & \text{(matching condition with zeroth-order inviscid core flow)}
\end{array}\right\} \tag{9}$$

Under the constant wall temperature, the solutions of Eqs. (7) satisfying the conditions (8) have been published by Yao and Catton (1976a,b) for Pr = 0.01, 1, 10 of the constant property flow and Pr = 8 of the water flow (variable viscosity). Their results will be summarized briefly below in order to make this report self-contained.

The dependent variables can be expressed as

$$w = f_0'(\eta) + \varepsilon(2z)^2 F_1'(\eta) \cdot \cos\phi + \ldots \tag{10a}$$

$$v = \varepsilon(2z) \cdot F_2'(\eta) \cdot \sin\phi + \ldots \tag{10b}$$

$$u = \frac{1}{\sqrt{2z}}(\eta f_0' - f_0) + \varepsilon(2z)^{3/2}(\eta F_1' - 5F_1 - F_2) \cdot \cos\phi + \ldots \tag{10c}$$

$$\theta = \theta_0(\eta) + \varepsilon(2z)^2 \cdot G(\eta) \cdot \cos\phi + \ldots \tag{10d}$$

where $\eta = \bar{r}/\sqrt{2z}$ is the Blasius variable. Substitution of Eqs. (10) into Eqs. (7) and collecting terms of equal order of ε yields

$$(N_0 f_0'')' + f_0 f_0'' = 0 \tag{11a}$$

$$\theta_0'' + \mathrm{Pr}\, f_0 \theta_0' = 0 \tag{11b}$$

and

$$\left.\begin{aligned} (N_0 F_1'')' + f_0 F_1'' - 4 f_0' F_1' - 5 f_0'' F_1 + f_0'' F_2 &= (A \cdot G \cdot f_0'')' \\ (N_0 F_2'')' + f_0 F_2'' - 2 f_0' F_2' &= -\theta_0 \\ \frac{1}{\mathrm{Pr}} G'' + f_0 G' - 4 f_0' G &= -\theta_0' (5F_1 + F_2) \end{aligned}\right\} \tag{12}$$

where

$$\left.\begin{aligned} N_0 &= \frac{1}{1 + \alpha(T_w - T_{in})\theta_0} \\ A &= \frac{-\alpha(T_w - T_{in})}{\left[1 + \alpha(T_w - T_{in})\theta_0\right]^2} \end{aligned}\right\} \tag{13}$$

and α is the coefficient of the variable viscosity. For water in the temperature range between 40°F (4.4°C) and 100°F (37.8°C), $\alpha \simeq 0.0151\ (°F)^{-1}$; for the constant property flow, $\alpha = 0$. The boundary conditions (9) become

$$\left.\begin{aligned} f_0 = f_0' = 0 \quad \text{and} \quad \theta_0 = 1 \quad \text{at} \quad \eta = 0 \\ f_0' \to 0 \quad \text{and} \quad \theta_0 \to 0 \quad \text{as} \quad \eta \to \infty \end{aligned}\right\} \tag{14a}$$

and

$$\left.\begin{aligned} F_1 = F_1' = F_2 = F_2' = G = 0 \quad &\text{at} \quad \eta = 0 \\ F_1',\ F_2',\ \text{and}\ G \to \infty \quad &\text{as} \quad \eta \to \infty \end{aligned}\right\} \tag{14b}$$

The numerical values of stream functions f_0, θ_0, F_1, F_2, and G can be found in Yao and Catton (1976a,b).

The velocity normal to the wall along the outer edge of the boundary layer is required to solve the second-order inviscid core flow (matching conditions). The matching conditions can be obtained by taking the limit of Eq. (10c) for $\eta \to \infty$, which gives

$$\begin{aligned} U_1(r = 1) = &- \lim_{\eta \to \infty} \left\{ \frac{1}{\sqrt{2z}} (\eta f_0' - f_0) + \varepsilon(2z)^{3/2} \right. \\ &\left. \times (\eta F_1' - 5F_1' - F_2) \cos\phi + \ldots \right\} \\ = &\frac{\beta_1}{\sqrt{2z}} - \varepsilon\beta_2(2z)^{3/2} \cos\phi + \ldots \end{aligned} \tag{15a}$$

where

$$\beta_1 = \lim_{\eta \to \infty} (\eta - f_0) \tag{15b}$$

$$\beta_2 = \lim_{\eta \to \infty} (5F_1 + F_2) \tag{15c}$$

The values of β_1 and β_2 for Pr = 0.01, 1.0, 10 of the constant property flow and for Pr = 8 of the water flow are taken from Yao and Catton (1976a,b) and are listed in Table 1.

Table 1

CONSTANTS FROM THE COMPUTATION OF THE BOUNDARY-LAYER FLOW

A. Constant T_w

Constant Property[a]				Variable Viscosity (Pr = 8)[b]			
β \ Pr	0.01	1.0	10.0	β \ αΔT	0	0.5	1
β_1	1.2167	1.2167	1.2167	β_1	1.2167	1.0617	0.9497
β_2	3.9454	0.8534	0.3158	β_2	0.3522	0.3106	0.2835

B. Constant q_w (constant property)

β \ Pr	0.01	1.0	10.0
β_1	1.2167	1.2167	1.2167
β_3	23.3511	0.9062	0.1524

[a]Yao and Catton, 1976a.

[b]Yao and Catton, 1976b.

For the case of constant wall heat flux, the dependent variables can be expanded as

$$w = f_0' + \varepsilon(2z)^{5/2} \cdot F_1' \cdot \cos\phi + \ldots \tag{16a}$$

$$v = \varepsilon(2z)^{3/2} \cdot F_2' \cdot \sin\phi + \ldots \tag{16b}$$

$$u = \frac{1}{\sqrt{2z}} (\eta f_0' - f_0) + \varepsilon(2z)^2 \cdot (\eta F_1' - 6F_1 - F_2) \cdot \cos\phi + \ldots \tag{16c}$$

$$\theta = \sqrt{2z} \cdot \theta_0 + \varepsilon(2z)^3 \cdot G \cdot \cos\phi + \ldots \tag{16d}$$

The governing equations for f_0, θ_0, F_1, F_2, and G are

$$\left.\begin{aligned} f_0''' + f_0 f_0'' &= 0 \qquad (17a)\\ \frac{1}{Pr}\,\theta_0'' + f_0\theta_0' - f_0'\theta_0 &= 0 \qquad (17b)\end{aligned}\right\}$$

$$\left.\begin{aligned} F_1''' + f_0 F_1'' - 5f_0' F_1' + 6f_0'' F_1 &= -f_0'' F_2 \qquad (17c)\\ F_2''' + f_0 F_2'' - 3f_0' F_2' &= -\theta_0 \qquad (17d)\\ \frac{1}{Pr}\,G'' + f_0 G' - 6f_0' G &= -\theta_0 F_1' - \theta_0'(6F_1 - F_2) \qquad (17e)\end{aligned}\right\}$$

The boundary conditions of Eqs. (18) for constant wall heat flux are

$$\left.\begin{aligned} f_0 = f_0' = 0, \quad \theta_0' = -1 \quad &\text{at} \quad \eta = 0\\ f_0' \to 1, \quad \theta_0 \to 0 \quad &\text{as} \quad \eta \to \infty\end{aligned}\right\} \qquad (18a)$$

and

$$\left.\begin{aligned} F_1 = F_1' = F_2 = F_2' = G' = 0 \quad &\text{at} \quad \eta = 0\\ F_1',\ F_2',\ G \to 0 \quad &\text{as} \quad \eta \to \infty\end{aligned}\right\} \qquad (18b)$$

The normal velocity along the outer edge of the boundary layer which is the matching condition for the second-order inviscid core flow is

$$U_1(r = 1) = -\frac{\beta_1}{\sqrt{2z}} + \beta_3 \cdot \varepsilon(2z)^2 \cdot \cos\phi + \ldots \qquad (19a)$$

where

$$\beta_3 = \lim_{\eta \to \infty} (6F_1 + F_2) \tag{19b}$$

is also listed in Table 1.

FIRST-ORDER INVISCID CORE FLOW

The equations of the first-order inviscid core flow are found by substituting Eqs. (4) and (5) into Eqs. (2). They are

$$\frac{1}{r}\frac{\partial(rU_1)}{\partial r} + \frac{1}{r}\frac{\partial V_1}{\partial \phi} + \frac{\partial W_1}{\partial z} = 0 \tag{20a}$$

$$\frac{\partial U_1}{\partial z} = -\frac{\partial P_1}{\partial r} + \varepsilon(\Theta_1 - \Theta_1^c)\cos\phi \tag{20b}$$

$$\frac{\partial V_1}{\partial z} = -\frac{\partial P_1}{r\,\partial \phi} + \varepsilon(\Theta_1 - \Theta_1^c)\sin\phi \tag{20c}$$

$$\frac{\partial W_1}{\partial z} = -\frac{\partial P_1}{\partial z} \tag{20d}$$

$$\frac{\partial \Theta_1}{\partial z} = 0 \tag{20e}$$

The temperature of the inviscid core flow, up to this order, is still not changed and is equal to the inlet temperature. This is confirmed by Eq. (20e), the solution of which is $\Theta_1 \equiv 0$. Therefore, there is no buoyancy force acting on the fluid in the central core of the pipe. Equations (20a) through (20d) can be separated into two parts: the accelerating axial flow due to the displacement effect of axial boundary layer and the downward stream due to the displacement effect of the secondary boundary layer. The equations governing the two phenomena are found by substituting

$$\left.\begin{aligned} U_1 &= U_{10} + \varepsilon U_{11} \cos\phi + \ldots \\ V_1 &= \varepsilon V_{11} \sin\phi + \ldots \\ W_1 &= W_{10} + \varepsilon W_{11} \cos\phi + \ldots \\ P_1 &= P_{10} + \varepsilon P_{11} \cos\phi + \ldots \end{aligned}\right\} \tag{21}$$

into Eqs. (20). After collecting the terms without ε and with ε, we have

$$\frac{1}{r}\frac{\partial(rU_{10})}{\partial r} + \frac{\partial W_{10}}{\partial z} = 0 \tag{22a}$$

$$\frac{\partial U_{10}}{\partial z} = -\frac{\partial P_{10}}{\partial r} \tag{22b}$$

$$\frac{\partial W_{10}}{\partial z} = -\frac{\partial P_{10}}{\partial z} \tag{22c}$$

and

$$\frac{1}{r}\frac{\partial(rU_{11})}{\partial r} + \frac{V_{11}}{r} + \frac{\partial W_{11}}{\partial z} = 0 \tag{23a}$$

$$\frac{\partial U_{11}}{\partial z} = -\frac{\partial P_{11}}{\partial r} \tag{23b}$$

$$\frac{\partial V_{11}}{\partial z} = \frac{P_{11}}{r} \tag{23c}$$

$$\frac{\partial W_{11}}{\partial z} = -\frac{\partial P_{11}}{\partial z} \tag{23d}$$

Displacement Effect $(O(\delta))$

The appropriate matching condition for Eqs. (22) is

$$U_{10} = - \beta_1/(2z)^{\frac{1}{2}} \qquad \text{at } r = 1 \tag{24a}$$

and the entry conditions are

$$P_{10} = W_{10} = 0 \qquad \text{at } z = 0 \tag{24b}$$

Integrating Eq. (22c) with respect to z and using (24a) gives

$$W_{10} = - P_{10} \tag{25}$$

Eliminating U_{10} and W_{10} from Eqs. (22a), (22b) and (25) results in

$$\frac{\partial^2 P_{10}}{\partial r^2} + \frac{1}{r}\frac{\partial P_{10}}{\partial r} + \frac{\partial^2 P_{10}}{\partial z^2} = 0 \tag{26}$$

The solution of Eq. (26) satisfying condition (24a) can be found by Fourier Transform in the sense of generalized functions (see Lighthill, 1958). It is

$$P_{10} = - \frac{\beta_1}{\sqrt{\pi}} \int_0^\infty \alpha^{-\frac{1}{2}} \frac{I_0(\alpha r)}{I_1(\alpha)} \sin \alpha z \, d\alpha \tag{27a}$$

where I's are modified Bessel functions.

Substituting Eq. (27a) into Eqs. (22b) and (22c), we obtain

$$W_{10} = \frac{\beta_1}{\sqrt{\pi}} \int_0^\infty \alpha^{-\frac{1}{2}} \frac{I_0(\alpha r)}{I_1(\alpha)} \sin \alpha z \, d\alpha \tag{27b}$$

and

$$U_{10} = - \frac{\beta_1}{\sqrt{\pi}} \int_0^\infty \alpha^{-\frac{1}{2}} \frac{I_1(\alpha r)}{I_1(\alpha)} (\cos \alpha z - 1) \, d\alpha \tag{27c}$$

The asymptotic values of Eqs. (27) for large z can be easily found:

$$W_{10} = - P_{10} = \beta_1 \cdot 2(2z)^{\frac{1}{2}} \cdot \left[1 + \tfrac{1}{4} \frac{r^2}{(2z)^2} + \ldots\right] \tag{28a}$$

$$U_{10} = - \beta_1 \cdot r \cdot (2z)^{-\frac{1}{2}} \tag{28b}$$

Equations (27) or (28) represent the accelerating flow due to the displacement effect of the boundary layer in an unheated pipe.

Secondary Displacement Effect $O(\delta\varepsilon)$

For the constant wall temperature, the matching condition for Eqs. (23) is found from Eqs. (15) and is

$$U_{11} = \beta_2 (2z)^{3/2} \qquad \text{at } r = 1 \tag{29a}$$

The entry conditions are

$$P_{11} = W_{11} = 0 \qquad \text{at } z = 0 \tag{29b}$$

Solving Eqs. (23) with conditions (29) yields

$$W_{11} = - P_{11} = - \frac{6\beta_2}{\sqrt{\pi}} \int_0^\infty \alpha^{-5/2} \frac{I_1(\alpha r)}{I_0(\alpha) + I_2(\alpha)} \sin \alpha z \cdot d\alpha \tag{30a}$$

$$V_{11} = - \frac{6\beta_2}{r\sqrt{\pi}} \int_0^\infty \alpha^{-5/2} \frac{I_1(\alpha r)}{I_0(\alpha) + I_2(\alpha)} (\cos \alpha z - 1)\, d\alpha \tag{30b}$$

and

$$U_{11} = - \frac{3\beta_2}{\sqrt{\pi}} \int_0^\infty \alpha^{-5/2} \frac{I_0(\alpha r) + I_2(\alpha r)}{I_0(\alpha) + I_2(\alpha)} (\cos \alpha z - 1)\, d\alpha \tag{30c}$$

For a large z, they can be approximated by

$$W_{11} = - P_{11} \sim 3\beta_2 \cdot r \cdot \left[(2z)^{\frac{1}{2}} + \tfrac{1}{2}\left(1 - \frac{r^2}{4}\right)(2z)^{-3/2} + \ldots \right] \tag{31a}$$

and

$$-V_{11} = U_{11} \sim \beta_2 (2z)^{3/2} + \ldots \tag{31b}$$

For the case of constant wall heat flux, the matching condition is, from Eqs. (19),

$$U_{11} = \beta_3 (2z)^2 \qquad \text{at } r = 1 \tag{32}$$

With conditions (29b) and (32), the solutions of Eqs. (23) are

$$W_{11} = - P_{11} = 32\beta_3 \int_0^\infty \alpha^{-1} \cdot \frac{I_1(\alpha r)}{I_0(\alpha) + I_2(\alpha)} \cdot \delta'(\alpha) \cdot \sin \alpha z \, d\alpha$$

$$= 4\beta_3 \, r(2z) \tag{33a}$$

$$V_{11} = - \beta_3 (2z)^2 \tag{33b}$$

$$U_{11} = \beta_3 (2z)^2 \tag{33c}$$

where $\delta'(\alpha)$ is the first derivative of the delta function.

The analysis can be extended systematically to obtain higher order terms of the solution in the boundary layer and the core. The temperature of the center core is not changed up to $0(\delta\varepsilon)$; however, the downward convection, $0(\delta\varepsilon)$, will carry the hotter fluid from the boundary ($- \pi/2 \leq \phi \leq \pi/2$) into the cooler core and will increase the temperature of the core flow. The small temperature variation is not considered in this report.

IV. RESULTS AND DISCUSSION

BOUNDARY-LAYER FLOW

A detailed discussion of the boundary-layer flow for the case of constant wall temperature can be found in Yao and Catton (1976a,b) and will not be repeated here.

For the case of constant wall heat flux, the numerical results of functions θ_0, G_1, F_1, F_1', F_2 and F_2' are plotted in Figs. 2-7. The values of θ_0 for the case of constant q_w are larger than those for the case of constant T_w. The wall temperature for the case of constant q_w increases downstream, and its values can be calculated from Eq. (16d). The values of θ_0 and G_1 for Pr = 0.01, 1.0, and 10 are listed in Table 2. In Fig. 3 the values of the perturbed temperature are positive near the wall and negative near the core for the case of constant q_w. For the case of constant T_w they are always negative and are not plotted, since their values are too small to be shown in the scale of Fig. 3. The stream-function F_1 shown in Fig. 4 indicates that their values are much larger than that for the case of constant T_w. The induced axial velocity profile has more profound effects for the case of constant q_w. Similarly, the buoyancy force induces stronger secondary flow at the constant wall heat flux than at the constant wall temperature shown in Figs. 6 and 7.

Table 2

COEFFICIENTS FOR WALL TEMPERATURE AND SHEAR STRESS

Pr	$\theta_0(0)$	G(0)	$F_1''(0)/f_0''(0)$	$F_2''(0)$
0.01	9.1173	4.6807	1.2085	7.1801
1.0	1.5409	1.0053	0.0990	0.7914
10.0	0.7087	0.0958	0.0198	0.2309

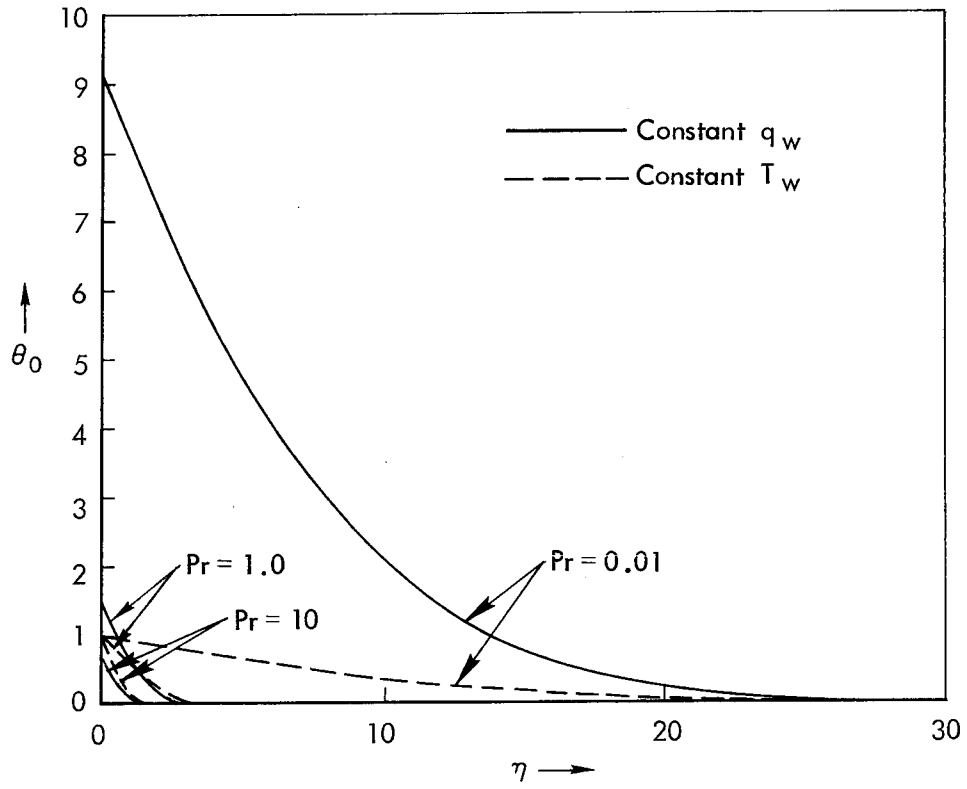

Fig. 2 — First-order temperature θ_0 (constant wall temperature and constant wall heat flux)

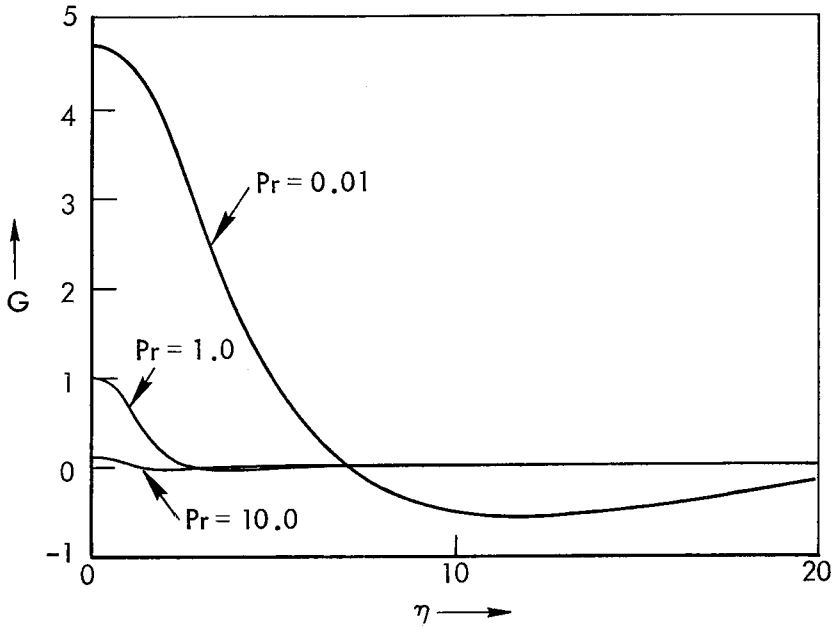

Fig. 3—Function G

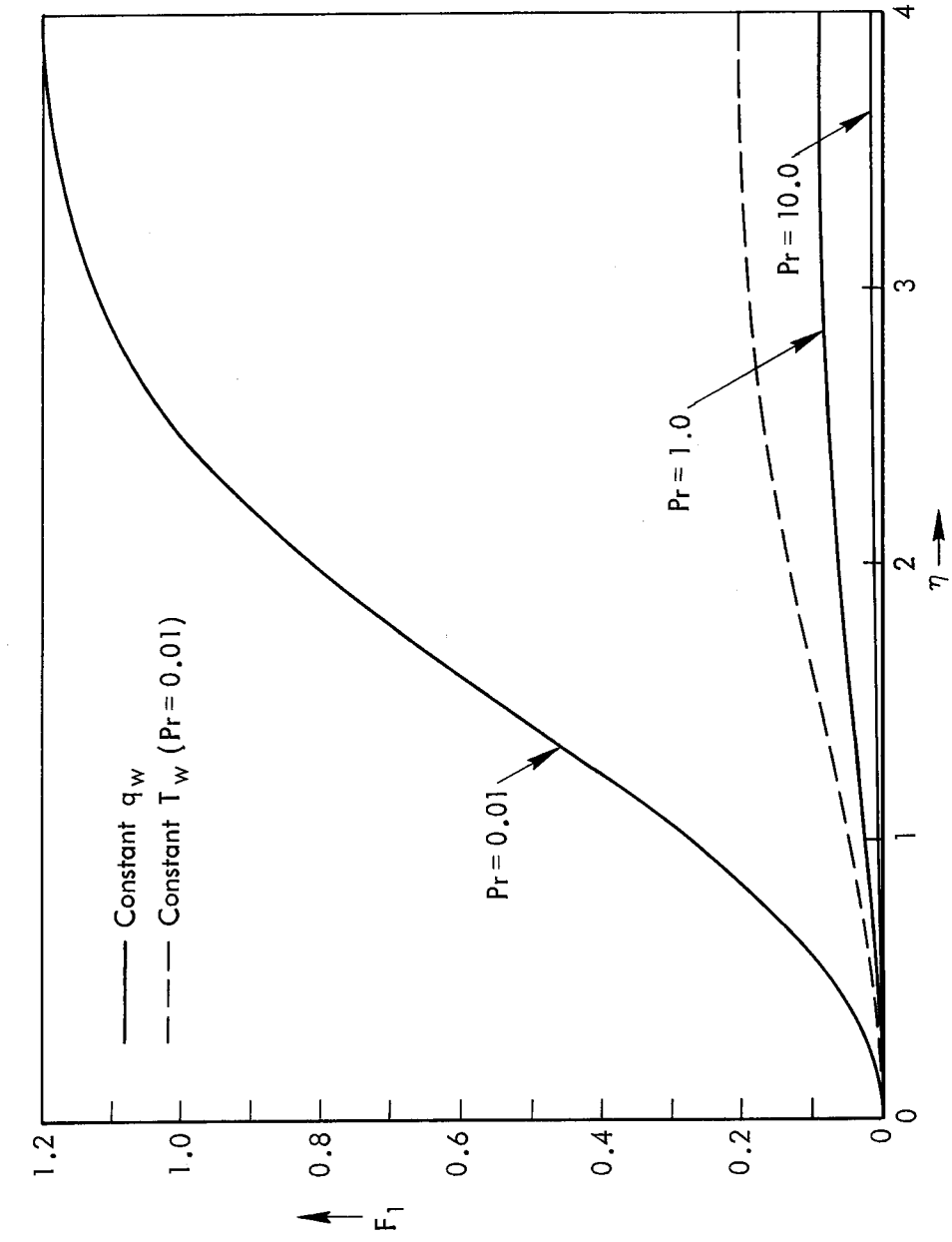

Fig. 4— Function F_1

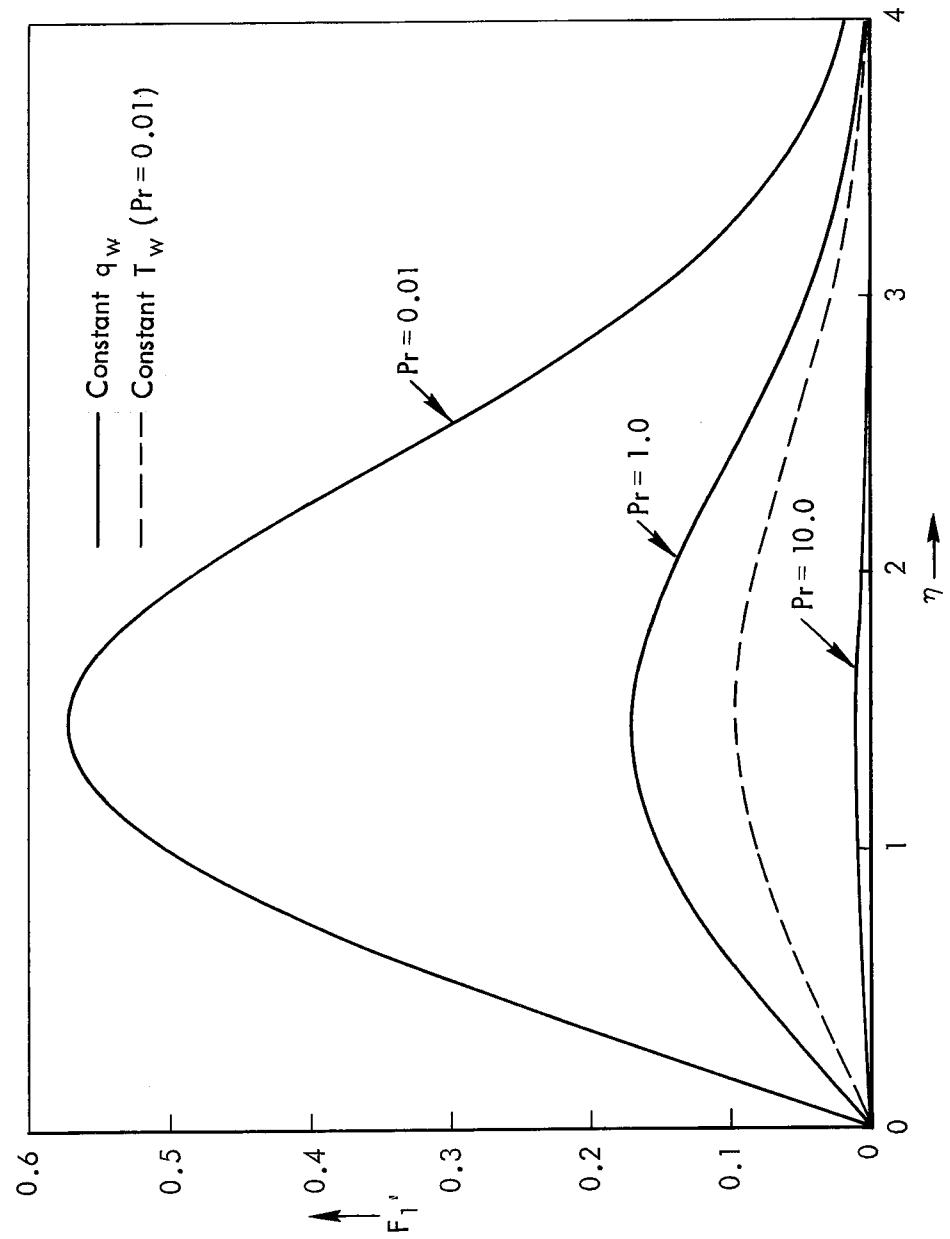

Fig. 5—Function F_1'

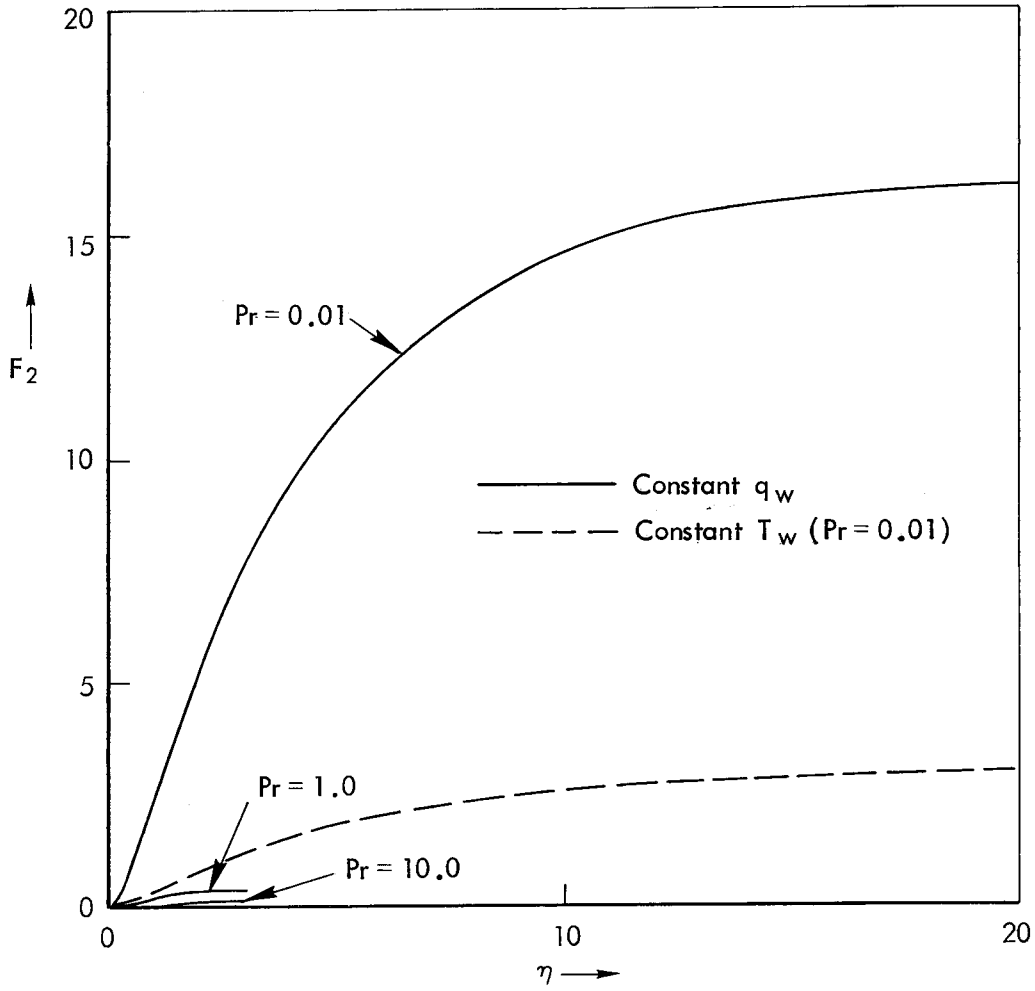

Fig. 6— Function F_2

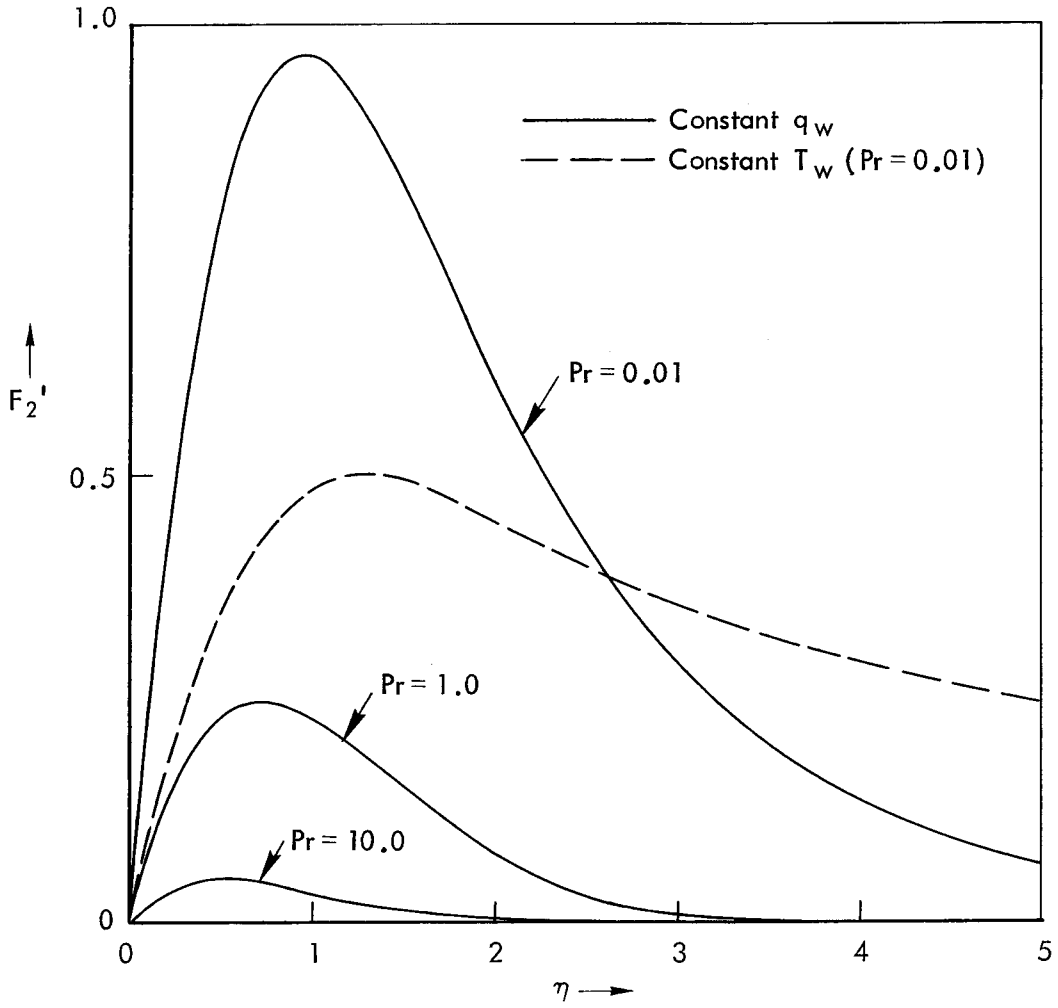

Fig. 7—Function F_2'

SHEAR STRESS

The local shear stress at the wall can be computed from the equation

$$\tau_{rz} = \mu \left.\frac{\partial w}{\partial r}\right|_{r=1} \quad \text{and} \quad \tau_{r\phi} = \mu \left.\frac{\partial v}{\partial r}\right|_{r=1}$$

Introducing the series expansions (16), the relative importance of the secondary flow on the axial shear stress can be found from

$$\frac{\tau_{rz}}{(\tau_{rz})_0} = 1 + \varepsilon(2z)^{5/2} \cdot \frac{F_1''(0)}{f_0''(0)} \cdot \cos\phi + \ldots \qquad (34)$$

The circumferential shear stress can be shown to be proportional to

$$\tau_{r\phi} \sim \varepsilon(2z)^{3/2} \cdot F_2''(0) \cdot \sin\phi \qquad (35)$$

Values of $F_1''(0)/f_0''(0)$ and $F_2''(0)$ are given in Table 2. Equations (16d) and (34) indicate that the secondary flow effect on the wall temperature and shear stress grows rapidly downstream, and is proportional to $z^{5/2}$. This means that an initially small secondary effect, which may be treated as a second-order effect in the region a distance O(a) from the inlet, becomes a dominant flow component farther downstream.

INVISCID CORE FLOW

Equations (27a,b) and (30a) are numerically integrated by using the Fast Fourier Transform. The details of the numerical method are described in Appendix A. W_{10}/β_1 (or $-P_{10}/\beta_1$) and W_{11}/β_2 (or $-P_{11}/\beta_2$) are evaluated at r = 0.5 as functions of z, and plotted in Fig. 8. The values of W_{10}/β_1 (or $-P_{10}/\beta_1$) at r = 0 differ only slightly from their values at r = 0.5 and are not present in the figure. Along the center line, functions W_{11} and P_{11} are identical to zero. W_{10} is the flow acceleration due to the displacement effect of the axial boundary layer. The flow is quickly accelerated near the entrance and the acceleration declines and is proportional to

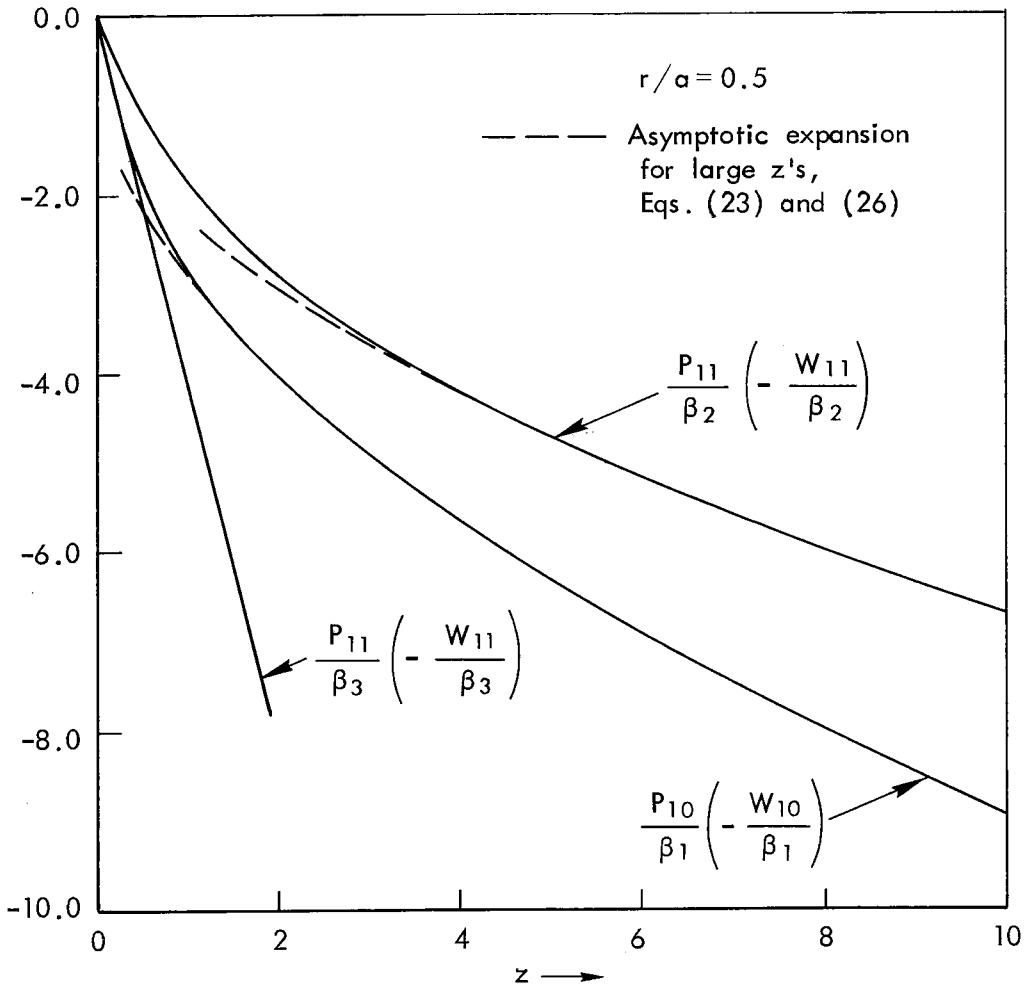

Fig. 8 — Displacement effect $\frac{W_{10}}{\beta_1}\left(\text{or } -\frac{P_{10}}{\beta_1}\right)$, and secondary flow effect $\frac{W_{11}}{\beta_2}\left(\text{or } \frac{P_{11}}{\beta_2}\right)$

$z^{-\frac{1}{2}}$ downstream. The distributions of W_{10} (or P_{10}) on the cross-section normal to the pipe axis are given in Fig. 9. Near the entrance z = 0.1, the axial velocity is higher close to the boundary layer than along the center line of the pipe. The delay of the flow acceleration near the center line causes the axial velocity profile to become concave. The velocity profile has its maximum velocity off the center line. The peaks are eroded downstream and eventually disappear at z = 2.5; see Fig. 9. A similar interpretation can be given to P_{10}, which is the pressure drop.

The displacement effects of the secondary boundary layer are represented by functions W_{11} and P_{11}. Physically, the secondary boundary layer causes the axial flow to turn counterclockwise around the horizontal line passing through the center of the pipe and normal to the axis of the pipe, Y = r cos ϕ = 0, and does not cause any net mean acceleration of the flow. The turning rate is higher near the entrance and gradually matches the rate which is proportional to $z^{-\frac{1}{2}}$.

For the case of contant T_w, the asymptotic expansions, Eqs. (28a) and (31a), of Eqs. (27a,b) and (30a) for large z's are also plotted in Fig. 8. They show that the asymptotic values of W_{10} (or P_{10}) match their exact value approximately at z = 2. For W_{11} (or P_{11}), the asymptotic values start to be valid at z = 4. The comparison of the asymptotic expansions with the exact evaluation of the sine integrals suggests that simpler asymptotic expansions can be used for practical application when z is larger than four, which will cover most ranges of practical interest when ε is small. The velocity components and the pressure, in terms of their asymptotic forms, are

$$P = -\delta \cdot (2z)^{\frac{1}{2}} \cdot \left\{ 2\beta_1 \left[1 + \frac{r^2 (2z)^{-2}}{4} + \ldots \right] + \varepsilon \cdot 3\beta_2 \cdot r \cos\phi \cdot \left[1 + \tfrac{1}{2}\left(1 - \frac{r^2}{4}\right)(2z)^{-2} + \ldots \right] \right\} \tag{36a}$$

$$W = 1 - P \tag{36b}$$

$$U = -\delta \cdot \left\{ \beta_1 \left[r(2z)^{-\frac{1}{2}} + \ldots \right] - \varepsilon\beta_2 \left[(2z)^{3/2} \cdot \cos\phi + \ldots \right] \right\} \tag{36c}$$

$$V = -\delta\varepsilon\beta_2 \left[(2z)^{3/2} \cdot \sin\phi + \ldots \right] \tag{36d}$$

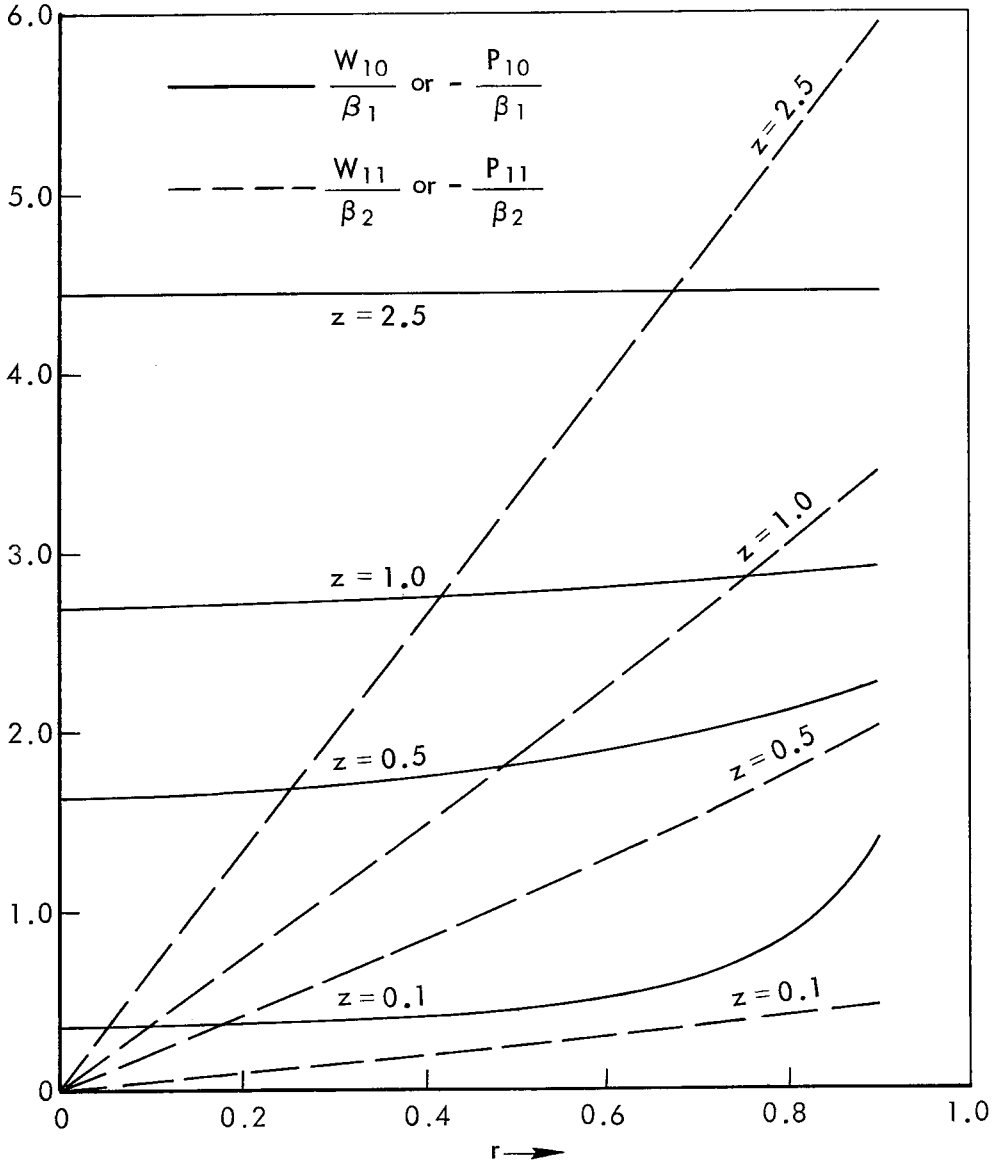

Fig. 9— Displacement effect: pressure $\frac{P_{10}}{\beta_1}$, velocity $\frac{W_{10}}{\beta_1}$, and secondary-flow effect: pressure $\frac{\tilde{P}_{11}}{\beta_2}$, velocity $\frac{\tilde{W}_{11}}{\beta_2}$ on the cross sections at $z = 0.1, 0.5, 1.0, 2.5$

For the case of constant q_w, the terms of $0(\delta\varepsilon)$ in Eqs. (36) are replaced by Eqs. (33).

PRESSURE DROP

The pressure head will drop along the pipe as the flow is accelerated. The first term of Eq. (36a) represents the pressure drop in an unheated pipe due to the displacement of the axial boundary layer. The pressure drops faster close to the edge of the boundary layer than along the center line of the pipe where r = 0. The difference in the pressure distribution on the cross-section of the pipe disappears for large z, and the pressure distribution approaches

$$P \sim -\delta \cdot 2\beta_1 (2z)^{\frac{1}{2}} \tag{37}$$

The pressure distribution is disturbed when the pipe wall is heated, which is represented by the second term of Eq. (36a). This term can be rewritten in $(\bar{X},\bar{Y},z)$ coordinates as $\delta\varepsilon\ 3\beta_2 Y(2z)^{\frac{1}{2}}$ for constant T_w, and as $\delta\varepsilon\ 8\beta_3\ Yz$ for constant q_w, which shows that the displacement effect of the secondary boundary layer introduces an unfavorable pressure gradient over the upper half of the pipe flow, Y > 0, and a favorable one over the lower half of the pipe, Y < 0.

AXIAL-VELOCITY PROFILES OF THE CORE FLOW

The axial velocity of the core flow can be viewed as a superposition of these components. The first one is the undisturbed flow at the inlet, i.e., W = 1. The second one is the accelerated flow due to the displacement effect of the axial boundary layer in an unheated pipe. The last component is due to the displacement of the secondary boundary layer. Similar to the pressure distribution, the third term in (X,Y,z) coordinates is $-\delta\varepsilon 3\beta_2 Y(2z)^{\frac{1}{2}}$ for constant T_w, and $-\delta\varepsilon\ 8\beta\ Yz$ for constant q_w, which means that the axial velocity profile turns counterclockwise around Y = 0. In the region of $z \sim 0(a)$, both the second and the third terms increase as $z^{\frac{1}{2}}$ for constant T_w, and as z for constant q_w. However, the second term may be dropped when the third term is still growing downstream beyond

the region of O(a) when Gr is not small. For the cases of small Gr (or ReGr), the second and the third terms will continue growing and the flow will approach its fully developed state.

VELOCITIES ON THE CROSS-SECTION

The radial velocity component U is given in Eq. (36c). The first term is due to the displacement effect of the axial boundary layer, which displaces the fluid away from the wall and toward the center of the pipe. The second term represents the motion when the fluid leaves the boundary layer over the upper half of the pipe ($\pi/2 < \phi < 3\pi/2$), and enters the boundary layer over the lower half of the pipe ($-\pi/2 < \phi < \pi/2$). The first kind of motion declines downstream, and the second one increases due to heating. They become the same order of magnitude when $z \sim O(a/\sqrt{\varepsilon})$ (or $O(a/\varepsilon^{2/5})$). Beyond this point, the analysis is no longer valid. For the case of large Gr, the second term becomes dominant and the axial length scale will be $a/\sqrt{\varepsilon}$ (or $a/\varepsilon^{2/5}$ for the constant q_w case). For a small Gr, $a/\sqrt{\varepsilon}$ (or $a/\varepsilon^{2/5}$ for the constant q_w case) is larger than a • Re. This suggests that the next length scale will be a • Re. Physically, it suggests that the flow development will be similar to the unheated, straight pipe and the solution of the slightly heated pipe can be obtained by perturbing the solution of an unheated pipe. Along the line of $\phi = 0$, where V = 0, there is a stagnation point at

$$r = \begin{cases} \dfrac{\beta_2}{\beta_1}\left[\varepsilon(2z)^2\right] & \text{(contant } T_w\text{)} \\ \dfrac{\beta_3}{\beta_1}\left[\varepsilon(2z)^{5/2}\right] & \text{(constant } q_w\text{)} \end{cases} \tag{38}$$

This is also a saddle point, point P in Fig. 10, which is similar to the entry flow of a curved pipe found by Singh (1974). In a heated pipe, $\varepsilon\beta_2/\beta_1$ (or $\varepsilon\beta_3/\beta_1$) is smaller than one, Table 1, and the analysis requires the quantity $\left[\varepsilon(2z)^2\right]$ to be smaller than one. Therefore, the saddle point P can never move into the boundary layer within the region of O(a).

Equation (36d) shows that the circumferential velocity has a maximum at $\phi = \pi/2$ and is equal to zero at both the top and the bottom of the pipe, $\phi = 0,\pi$.

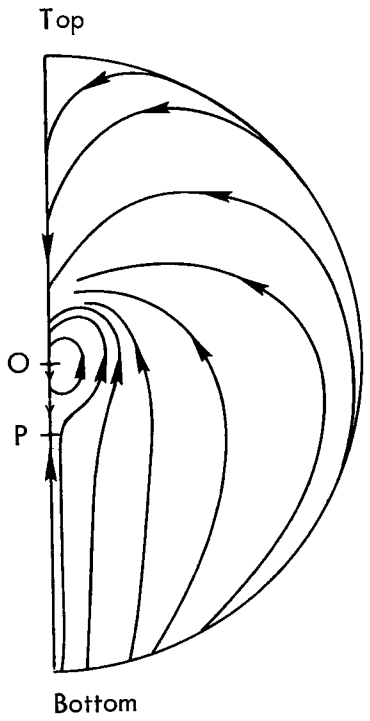

Fig. 10— Streamlines on the cross section

STREAMLINES ON THE CROSS-SECTION

For constant T_w, the projection of the streamline on a cross-section can be computed by

$$\frac{1}{r}\frac{dr}{d\phi} = \frac{\beta_1 r(2z)^{-\frac{1}{2}} - \varepsilon\beta_2 \cos\phi(2z)^{3/2}}{\varepsilon\beta_2 \sin\phi(2z)^{3/2}} \tag{39}$$

Equation (39) shows that all streamlines are tangent to the vertical line, $\phi = 0,\pi$, and are plotted in Fig. 10. If z is not too large, the second term in the numerator of Eq. (39) can be neglected and Eq. (39) can be integrated to give

$$\tan \frac{\phi}{2} = e^{-\frac{\varepsilon \beta_2 (2z)^2}{\beta_1 r}} + \text{constant} \tag{40}$$

For $\varepsilon = 0$, an unheated straight pipe, Eq. (40) becomes ϕ = constant. The streamlines on the cross-section are a radial straight line. Within the limit of the analysis, the second term on the numerator of Eq. (39) can never be larger than the first one. Nevertheless, stretching our interpretation of Eq. (39) somewhat and considering it for large z can predict what may occur for the flow development farther downstream. Equation (39) becomes, after neglecting the first term of the numerator and integrating,

$$\bar{x} = \text{constant} \tag{41}$$

which shows that the streamlines on the cross-section, due to the displacement effect of the secondary boundary layer, are vertical straight lines. The magnitude of this downward flow is

$$\sqrt{U_{11}^2 + V_{11}^2} = \beta_2 (2z)^{3/2} \tag{42}$$

which increase downstream. This flow, when Gr is large, will eventually become the dominant flow pattern, which is observed by Mori and Futagami (1967). Also, the downward stream forms a stagnation-like flow locally along the bottom wall of the pipe. The convective effect of this locally stagnant flow prevents the boundary layer from growing. Thus, the boundary layer will remain thin as the flow moves downstream. Therefore, the flow acceleration due to the displacement effect of the axial boundary layer will fade out. This suggests that the flow development in the region of $0(a/\sqrt{\varepsilon})$ (or $0(a/\varepsilon^{2/5})$) is mainly in changing the slope of the axial velocity profile to balance the gradually enhanced flow in the secondary boundary layer. Also, the unfavorable pressure gradient near the top wall of the pipe gradually grows and eventually triggers the separation of the boundary layer farther downstream. The phenomenon of the flow development will be similar to that of a curved pipe given by Yao and Berger (1975). A similar interpretation can be made for the case of constant q_w.

V. THE TUBE TEST IN COLORADO (Barker and Jennings, 1977)

The dimensions of the tube used in Colorado are shown in Fig. 11. The heating condition is assumed to be constant wall temperature. The range of Re, Gr, and ε are computed on the basis of the preliminary test arrangement:

$$T_{in} = 52°F$$

$$\alpha = 0.0151\ (°F)^{-1}$$

$$\gamma = 0.49 \times 10^{-4}\ (°F)^{-1}$$

$$a = 2" = 0.167'$$

$$g = 32.2\ ft/sec^2$$

$$\nu = 1.31 \times 10^{-5}\ ft^2/sec$$

$$Pr = 8$$

$$W_{in} = 5 - 30\ ft/sec$$

$$\Delta T = T_w - T_{in} = 0 - 40°$$

$$Re = \frac{W_{in} a}{\nu} = 1.27 \times 10^5 - 1.02 \times 10^6$$

$$Gr = \frac{\gamma g a^3 \Delta T}{\nu^2} = 0 - 3.49 \times 10^6$$

$$\varepsilon = \frac{Gr}{Re^2} = 0 - 2.17 \times 10^{-4}$$

$$\delta = \frac{1}{\sqrt{Re}} = 9.90 \times 10^{-4} - 2.81 \times 10^{-3}$$

From the previous section we know that the secondary flows induced by the buoyancy forces are $0(\delta\varepsilon)$ in the core flow and $0(\varepsilon)$ in the boundary-layer flow; these are very small in the region distance $0(a)$ from the entrance, and can be neglected. The test data obtained in the region can be interpreted as being equivalent to what would be obtained for an exterior flow, except that there is a slight acceleration of the flow due

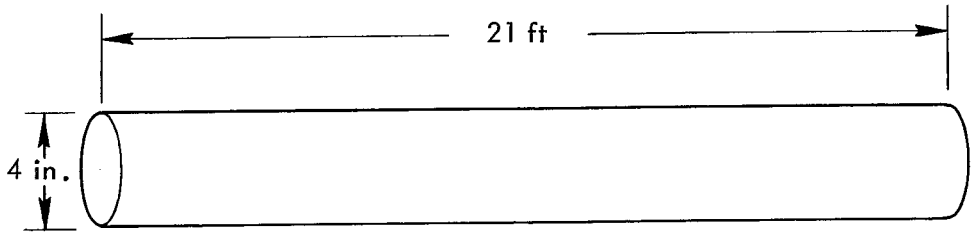

$W_{in} = 5 \sim 30$ ft/sec

$T_{in} = 52°F$

$T_w - T_{in} = 0 \sim 40°F$

Fig. 11 — Tube test in Colorado

to the displacement of the axial boundary layer. The flow acceleration can be calculated from Eq. (36b), which is, for z = 4,

$$\Delta W = \frac{W - W_{in}}{W_{in}} = \delta \cdot \beta_1 2(2z)^{\frac{1}{2}} \tag{43}$$

The range of ΔW for 21-ft- and 45-ft-long pipes is given in Table 3.

Table 3

FLOW ACCELERATION

(Pr = 8)

$\alpha\Delta T$ \ ΔW	21-ft pipe (%)	45-ft pipe (%)
0	1.52 - 4.32	2.29 - 6.49
0.5	1.33 - 3.77	1.99 - 5.66
1	1.19 - 3.37	1.78 - 5.61

which shows that the flow acceleration decreases when the heating rate increases. The upper bound of the flow acceleration is about 6.5 percent.

In general, the flow acceleration will stabilize the boundary layer; the quantification of this effect is being studied and will be reported when it is completed.

In view of the above examination, the data obtained from the tube test will be valuable in simulating external flow if the flow region in the tube falls in the solution of the region distance $0(a)$ from the entrance. However, the size of the region $0(a)$, the solution of which is presented in the previous sections, is determined by the magnitude of ε. From a preliminary investigation of the next region, distance $0(aRe/Gr^{\frac{1}{2}})$ from the entrance, it is indicated that the size of the region $0(a)$ is about

$$z < \frac{0.46}{\sqrt{\varepsilon}} = \frac{0.46W_{in}}{\sqrt{\gamma g a \Delta T}} \sim 28.36 \frac{W_{in}}{\sqrt{\Delta T}} \tag{44}$$

This shows the size of the region distance $0(a)$ from the entrance is about 7.5 ft from the entrance when the inlet velocity is 10 ft/sec and $\Delta T = 40°F$ (condition I). This distance increases when the inlet velocity increases and ΔT decreases. Its value equals approximately 44.9 ft from the entrance when the inlet velocity = 30 ft/sec and $\Delta T = 10°F$ (condition II). Therefore, under condition II, the flow in the test tube is governed by the solutions presented in the previous section and can be used to model the external flow. However, under condition I, only the flow of the first 7.5 ft from the entrance of the test tube can be used to simulate the exterior flow. From 7.5 ft to the exit of the tube, the flow is governed by the solution of the region distance $0(aRe/Gr^{\frac{1}{2}})$ from the entrance, since the values of Gr are large in those tests.

From the tube test in Colorado, it has been found that it is necessary to increase the wall temperature and the flow rate simultaneously in order to obtain the maximum wall-heating effect on the flow transition. Otherwise, the measured transition Reynolds number was inevitably much lower. This is apparent because the "overheating" causes strong secondary flow and destabilizes the boundary layer. This phenomenon is demonstrated in Fig. 12. The dot-circles are the "successful" data

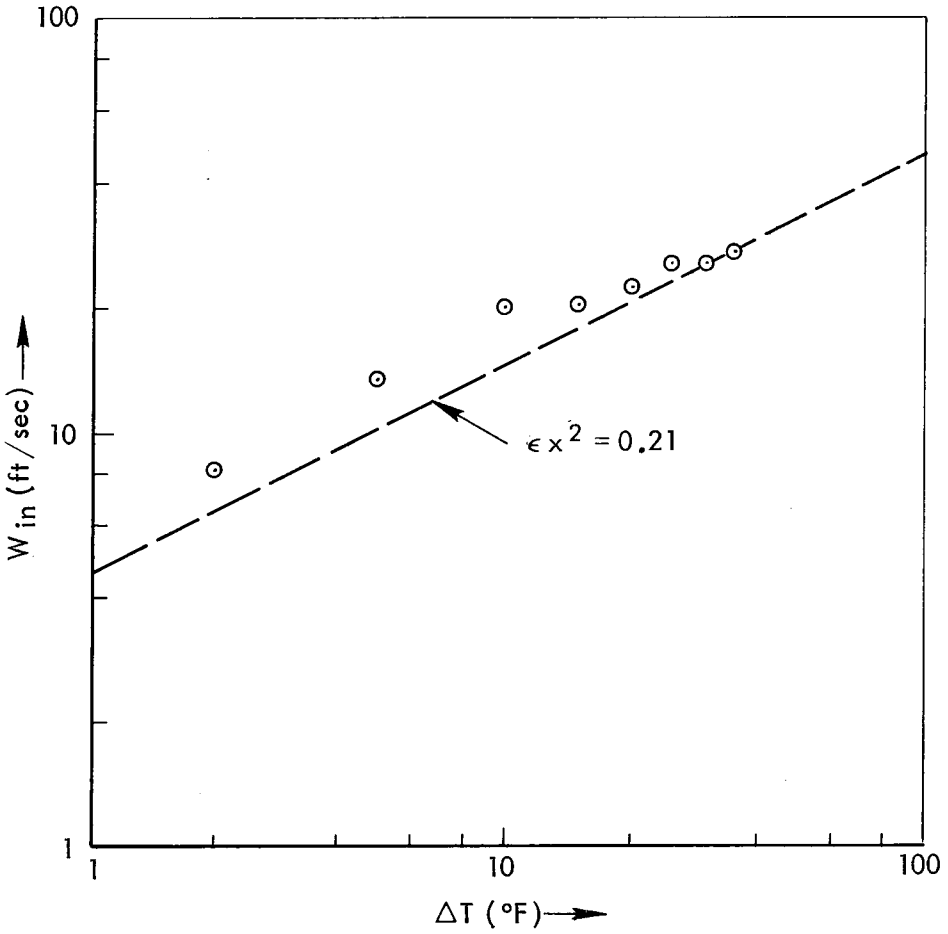

Fig. 12— Laminar path

from the tube test, and the two straight lines indicate the possible location of the end of the region of 0(a), where the buoyancy is expected to be negligible. The value $\varepsilon x^2 = 0.21$ is the line beyond which the buoyancy effect becomes important. Physically, the slope of the line can be viewed as the "slope" of the "laminar path." A preliminary analysis* indicates that the experimental data $\Delta T \leq 10°F$ compared reasonably with the theoretical prediction. However, the data for $\Delta T > 10°F$ are far below the theoretical estimation. The reason is quite clear, from Fig. 12: the experiments for $\Delta T > 10°F$ did not follow the slope of the laminar path and turned toward the buoyancy-dominant direction. The data for $\Delta T > 10°F$ are affected by the buoyancy forces; therefore, they are far below the theoretical predicted values.

The study of the developing flow in the region of $0(aRe/Gr^{\frac{1}{2}})$ is just being undertaken, and will be reported separately when it is completed. The intuitive expectation on the flow development in the region of $0(aRe/Gr^{\frac{1}{2}})$ would be that the unfavorable pressure gradient developed on the top wall of the pipe can cause flow separation and possibly trigger early flow transition. Especially, the size of the region 0(a) shrinks when the heating rate increases.

---

*Personal communication from Carl Gazley, Jr., The Rand Corporation.

Appendix A
NUMERICAL INTEGRATION OF SINE INTEGRALS

The integrals of Eqs. (27) and (30a) can be put in the general form of

$$\int_0^\infty F(\alpha) \sin \alpha z \, d\alpha \tag{A-1}$$

where $F(\alpha)$ may have integrable singularity at $\alpha = 0$. The integral (A-1) can be separated into two parts:

From $0 - \pi/z$

$$I = \int_0^{\pi/z} \left[F(\alpha) \sin \alpha z - G\alpha^{-\frac{1}{2}}\right] d\alpha + G \int_0^{\pi/z} \alpha^{-\frac{1}{2}} \, d\alpha \tag{A-2}$$

where

$$G = \lim_{\alpha \to 0} F(\alpha) \cdot \alpha^{\frac{1}{2}} \tag{A-3}$$

From $\pi/z - \infty$

$$\begin{aligned} II &= \int_{\pi/z}^\infty F(\alpha) \sin \alpha z \, d\alpha \\ &= \frac{1}{z} \sum_{k=1}^\infty \int_{k\pi}^{(k+1)\pi} F\left(\frac{\alpha}{z}\right) \cdot \sin \alpha \cdot d\alpha \\ &= \frac{1}{z} \int_0^\pi \sin \alpha \cdot \left[\sum_{k=1}^\infty (-1)^k \cdot F\left(\frac{\alpha + k\pi}{z}\right)\right] \cdot d\alpha \end{aligned} \tag{A-4}$$

The infinite series in (A-4) is summed by using Euler's transform, such as

$$\sum_{k=1}^{\infty} (-1)^k \cdot F\left(\frac{\alpha + k\pi}{z}\right) = \sum_{k=1}^{N} (-1)^k F\left(\frac{\alpha + k\pi}{z}\right) + (-1)^{N+1} \cdot \sum_{k=0}^{M} \frac{(-1)^k}{z^{k+1}} \left(\Delta^k u_0\right) \tag{A-5}$$

where

$$\left.\begin{aligned} u_0 &= F\left(\frac{\alpha + (N+1)\pi}{z}\right) \\ \Delta u_k &= u_{k+1} - u_k \end{aligned}\right\} \tag{A-6}$$

to speed the convergence of the summation. N = 30 and M = 10 are used to generate data which, we found, are far more than sufficient.

Equations (A-2) and (A-3) are numerically integrated by using Gaussian quadrature. After comparing the results, we found that either ten terms or sixteen terms gives sufficient accuracy. We use sixteen terms.

The computer program is listed in Appendix B.

Appendix B

COMPUTER PROGRAM

```
//Y1670LSY JOB (5472,150,Y,15),'LSYAO',CLASS=D                          0001
//COMP EXEC FORTCG,REGION.GO=70K,LIBL='SYS1.FORTEBP'                    0002
//FORT.SYSIN DD *                                                       0003
C*     PROGRAM PIPE(FAST FOURIER TRANSFORM) NOV. 5, 1976                0004
C*     THE ENTRANCE FLOW IN A HEATED PIPE                               0005
C*     THE SOLUTION COVERS Z=O(A)                                       0006
C                                                                       0007
      IMPLICIT REAL*8(A-H,O-Z),REAL*4($)                                0008
      DIMENSION G(50),U(10),H16(16),X16(16),H10(10),X10(10),H(16),XA(16) 0009
      COMMON PAI                                                        0010
      DATA NDG,NDU,NDH/50,10,16/                                        0011
      DATA H16/0.027152459411754D0,                                     0012
     1          0.027152459411754D0,                                    0013
     2          0.062253523938648D0,                                    0014
     3          0.062253523938648D0,                                    0015
     4          0.095158511682493D0,                                    0016
     5          0.095158511682493D0,                                    0017
     6          0.124628971255534D0,                                    0018
     7          0.124628971255534D0,                                    0019
     8          0.149595988816577D0,                                    0020
     9          0.149595988816577D0,                                    0021
     A          0.169156519395003D0,                                    0022
     B          0.169156519395003D0,                                    0023
     C          0.182603415044924D0,                                    0024
     D          0.182603415044924D0,                                    0025
     E          0.189450610455068D0,                                    0026
     F          0.189450610455068D0/                                    0027
C                                                                       0028
      DATA X16/0.989400934991650D0,                                     0029
     1         -0.989400934991650D0,                                    0030
     2          0.944575023073233D0,                                    0031
     3         -0.944575023073233D0,                                    0032
     4          0.865631202387832D0,                                    0033
     5         -0.865631202387832D0,                                    0034
     6          0.755404408355003D0,                                    0035
     7         -0.755404408355003D0,                                    0036
     8          0.617876244402644D0,                                    0037
     9         -0.617876244402644D0,                                    0038
     A          0.458016777657227D0,                                    0039
     B         -0.458016777657227D0,                                    0040
     C          0.281603550779259D0,                                    0041
     D         -0.281603550779259D0,                                    0042
     E          0.095012509837637D0,                                    0043
     F         -0.095012509837637D0/                                    0044
C                                                                       0045
C     DATA H10/0.066671344308688D0,                                     0046
C    1         0.066671344308688D0,                                     0047
C    2         0.149451349150581D0,                                     0048
C    3         0.149451349150581D0,                                     0049
C    4         0.219086362515982D0,                                     0050
C    5         0.219086362515982D0,                                     0051
C    6         0.269266719309996D0,                                     0052
C    7         0.269266719309996D0,                                     0053
C    8         0.295524224714753D0,                                     0054
C    9         0.295524224714753D0/                                     0055
C                                                                       0056
C     DATA X10/0.973906528517172D0,                                     0057
C    1         -0.973906528517172D0,                                    0058
C    2          0.865063366688985D0,                                    0059
C    3         -0.865063366688985D0,                                    0060
C    4          0.679409568299024D0,                                    0061
```

```
C     5         -0.6794095682990240D0,                                    0062
C     6          0.4333953941292470D0,                                    0063
C     7         -0.4333953941292470D0,                                    0064
C     8          0.1488743389816310D0,                                    0065
C     9         -0.1488743389816310D0/                                    0066
C                                                                         0067
C*     N=NO. OF TERMS FOR GAUSSIAN QUADRATURE                             0068
C*     NG+NE=NO OF TERMS FOR THE INFINITE SERIES                          0069
C*     H= WEIGHTONG FUNCTION FOR GAUSSIAN QUADRATURE                      0070
C*     XA=LOCATION FOR GAUSSIAN QUADRATURE                                0071
       CALL ERRSET(208,256,-1,1,1)                                        0072
       NC=0                                                               0073
 1001  NC=NC+1                                                            0074
       READ 101, R,Z,NSE                                                  0075
       PRINT 204, NC,R,Z                                                  0076
       PAI=3.141592654D0                                                  0077
       SQRPAI=DSQRT(PAI)                                                  0078
       A=PAI/Z                                                            0079
C                                                                         0080
C      N=10                                                               0081
C      NG=20                                                              0082
C      NE=5                                                               0083
C      DO 10 I=1,N                                                        0084
C      H(I)=H10(I)                                                        0085
C   10 XA(I)=X10(I)                                                       0086
C      GO TO 1003                                                         0087
 1002  N=16                                                               0088
       NG=30                                                              0089
       NE=10                                                              0090
       DO 20 I=1,N                                                        0091
       H(I)=H16(I)                                                        0092
    20 XA(I)=X16(I)                                                       0093
       NSE=NSE+1                                                          0094
C                                                                         0095
C*                                                                        0096
C*     INTEGRATION OF P10                                                 0097
C:                                                                        0098
 1003  CALL SIMP(N,A,R,Z,P101,1,G,U,H,XA,NDG,NDU,NDH)                     0099
       CALL GAUSS(N,NG,NE,R,Z,P102,2,G,U,H,XA,NDG,NDU,NDH)                0100
       P10=4.*Z*DSQRT(A)+P101+P102                                        0101
       P10=-1./SQRPAI*P10                                                 0102
       ASP10=-2.*DSQRT(2.*Z)*(1.+0.25*R*R/4./Z**2)                        0103
       PRINT 201, P101,P102                                               0104
C:                                                                        0105
C*     INTEGRATION OF P11 (CROSS-FLOW EFFECT)                             0106
C*                                                                        0107
       CALL SIMP(N,A,R,Z,P111,3,G,U,H,XA,NDG,NDU,NDH)                     0108
       CALL GAUSS(N,NG,NE,R,Z,P112,4,G,U,H,XA,NDG,NDU,NDH)                0109
       P11=R*Z*DSQRT(A)+P111+P112                                         0110
       P11=-6./SQRPAI*P11                                                 0111
       ASP11=-3.*R*(DSQRT(2.*Z)+0.5*(1.-0.25*R*R)/(2.*Z)**1.5)            0112
       PRINT 202, P111,P112                                               0113
       PRINT 203, P10,ASP10,P11,ASP11                                     0114
  101  FORMAT (2D10.3,I10)                                                0115
  204  FORMAT (I10//5X,'( R, Z )= ( ',D14.6,' , ',D14.6,' )')            0116
  201  FORMAT (/5X,'P10(0-A)=',D14.6,2X,'P10(A-XF)=',D14.6/)              0117
  202  FORMAT(5X,'P11(0-A)=',D14.6,2X,'P11(A-XF)=',D14.6/)                0118
  203  FORMAT (12X,'***  RESULT ***'//2X,'DISPLACEMENT EFFECT, P10= ',    0119
     1D14.6,'  ASP10= ',D14.6/4X,'CROSS-FLOW EFFECT, P11= ',              0120
     2D14.6,'  ASP11= ',D14.6///)                                        0121
C                                                                         0122
```

```
C     IF ( NSE.EQ.1 ) GO TO 1002                                        0123
C                                                                       0124
      GO TO 1001                                                        0125
      END                                                               0126
```

```
      SUBROUTINE SIMP(N,A,R,Z,TOTAL,NF,G,U,H,XA,NDG,NDU,NDH)          0127
C*                                                                    0128
C*    NF  = 1 OR 3                                                    0129
      IMPLICIT REAL*8(A-H,O-Z),REAL*4($)                              0130
      DIMENSION G(NDG),U(NDU),H(NDH),XA(NDH)                          0131
      COMMON PAI                                                      0132
      A2=.5*A                                                         0133
      TOTAL=0.                                                        0134
      DO 10 I=1,N                                                     0135
      Y=A2*(XA(I)+1.)                                                 0136
      CALL FUNC(Y,R,Z,FA,NF)                                          0137
   10 TOTAL=TOTAL+H(I)*FA                                             0138
      TOTAL=TOTAL*A2                                                  0139
      RETURN                                                          0140
      END                                                             0141
```

```
      SUBROUTINE GAUSS(N,NG,NE,R,Z,SUM1,NF,G,U,H,XA,NDG,NDU,NDH)
C*    INTEGRATION FROM 0. TO INFINITE
C*    N=NO. OF TERMS FOR GAUSS
C*    NG+NE=NO. OF TERMS FO SERIES
C*    NF=3 OR 4
      IMPLICIT REAL*8(A-H,O-Z),REAL*4($)
      DIMENSION G(NDG),U(NDU),H(NDH),XA(NDH)
      COMMON PAI
C***  GAUSSIAN QUADRATURE
      SUM1=0.
      A2=.5*PAI
      DO 50 I=1,N
      Y=A2*(1.+XA(I))
      G(I)=0.
      DO 10 K=1,NG
      YY=(Y+K*PAI)/Z
      CALL FUNC(YY,R,Z,F,NF)
      K1=MOD(K,2)
      G(I)=G(I)+(-1.)**K1*F
      GSUM=G(I)
      IF ( G(I).EQ.0.D0 ) GSUM=1.D0
      ERR=DABS(F/GSUM)
      IF (ERR.LE.1.D-10) GO TO 50
   10 CONTINUE
C*    EULER'S TRANSFORM
      DO 20 K=1,NE
      YY=(Y+(NG+1+K)*PAI)/Z
      CALL FUNC(YY,R,Z,F,NF)
   20 U(K)=F
      DO 30 L=2,NE
      DO 30 K=L,NE
   30 U(K)=U(K)-U(K-1)
      SUM=0.
      DG=1.D0
      DO 40 K=1,NE
      KG=MOD(K,2)
      DG=2.*DG
   40 SUM=SUM-(-1.)**KG/DG*U(K)
C     PRINT 201, NF,I,R,Z,G(I),SUM,ERR
      KG=MOD(NG,2)+1
      G(I)=G(I)+(-1.)**KG*SUM
   50 SUM1=SUM1+H(I)*DSIN(Y)*G(I)
      SUM1=SUM1*A2/Z
      RETURN
C 201 FORMAT (/2X,'GAUSS ** NF,I,R,Z,G(I),SUM,ERR = **'/
C    1        2I5,5D16.6/)
      END
```

```
      SUBROUTINE FUNC (XK,R,Z,F,N)                                      0189
      IMPLICIT REAL*8(A-H,O-Z),REAL*4($)                                0190
      RXK=R*XK                                                          0191
      ZXK=Z*XK                                                          0192
      CALL BESSEL (XK,B0,B1,B2)                                         0193
      CALL BESSEL (RXK,BB0,BB1,BB2)                                     0194
      X=XK                                                              0195
      IF (XK.EQ.0.) X=1.                                                0196
      SXK=1./DSQRT(X)                                                   0197
      EXK=XK*(R-1.D0)                                                   0198
      FAC=DEXP(EXK)                                                     0199
      IF (N.GT.2) GO TO 1003                                            0200
      F=FAC*BB0/B1                                                      0201
      IF (N.EQ.1) F=F*DSIN(ZXK)-2.*Z                                    0202
      F=F*SXK                                                           0203
      RETURN                                                            0204
1003  F=FAC*BB1/(B0+B2)                                                 0205
      IF (N.EQ.3) F=F*DSIN(ZXK)-0.5*R*Z*XK**2                           0206
      F=F*SXK/X**2                                                      0207
      RETURN                                                            0208
      END                                                               0209
```

```
      SUBROUTINE BESSEL (XK,B0,B1,B2)                                   0210
      IMPLICIT REAL*8(A-H,O-Z),REAL*4($)                                0211
C*    B(XK)=BESSEL(XK)*EXP(-XK)                                         0212
      IF (XK.EQ.0.0D0) GO TO 1002                                       0213
      KMAX=15                                                           0214
      NMAX=10                                                           0215
      B0=1.                                                             0216
      B1=1.                                                             0217
      F0=1.                                                             0218
      F1=1.                                                             0219
      IF (XK.GT.10.) GO TO 1001                                         0220
      X=XK*XK/4.                                                        0221
      DO 10 K=1,KMAX                                                    0222
      F0=F0*X/K/K                                                       0223
      F1=F1*X/K/(K+1)                                                   0224
      B0=B0+F0                                                          0225
   10 B1=B1+F1                                                          0226
      B1=B1*XK*0.5                                                      0227
      B0=B0*DEXP(-XK)                                                   0228
      B1=B1*DEXP(-XK)                                                   0229
      GO TO 30                                                          0230
 1001 X=8.*XK                                                           0231
      DO 20 K=2,NMAX                                                    0232
      RK3=2.*K-3.                                                       0233
      RK3=RK3**2                                                        0234
      F0=F0*RK3/(K-1)/X                                                 0235
      F1=F1*(-1.)*(4.-RK3)/(K-1)/X                                      0236
      B0=B0+F0                                                          0237
   20 B1=B1+F1                                                          0238
      DEN=1.D0/DSQRT(2.*3.14159*XK)                                     0239
      B0=B0*DEN                                                         0240
      B1=B1*DEN                                                         0241
   30 B2=B0-2./XK*B1                                                    0242
      RETURN                                                            0243
 1002 B0=1.                                                             0244
      B1=0.                                                             0245
      B2=0.                                                             0246
      RETURN                                                            0247
      END                                                               0248
/*                                                                      0249
//GO.SYSIN DD *                                                         0250
.5        .5                                                            0251
.5        10.                                                           0252
/*                                                                      0253
```

```
        1

    ( R, Z )= (   0.500000D 00 ,   0.500000D 00 )

    P10(0-A)= -0.179311D 01  P10(A-XF)= -0.231896D-01

    P11(0-A)= -0.316886D 00  P11(A-XF)= -0.161142D-03

           ***  RESULT ***

 DISPLACEMENT EFFECT, P10=  -0.180369D 01  ASP10=  -0.212500D 01
   CROSS-FLOW EFFECT, P11=  -0.104807D 01  ASP11=  -0.220313D 01


        2

    ( R, Z )= (   0.500000D 00 ,   0.100000D 02 )

    P10(0-A)= -0.566021D 01  P10(A-XF)= -0.912196D 00

    P11(0-A)= -0.712876D 00  P11(A-XF)= -0.109694D 00

           ***  RESULT ***

 DISPLACEMENT EFFECT, P10=  -0.894103D 01  ASP10=  -0.894567D 01
   CROSS-FLOW EFFECT, P11=  -0.670232D 01  ASP11=  -0.671607D 01


IHC900I EXECUTION TERMINATING DUE TO ERROR COUNT FOR ERROR NUMBER  217

IHC217I FIOCS - END OF DATA SET ON UNIT    5

TRACEBACK  ROUTINE  CALLED FROM ISN   REG.  14   REG.  15   REG.   0   REG.   1

           IBCOM                      0018C0F4   0018DF98   00000003   0018B9C8

           MAIN                       00014612   0118B810   FF000018   0019C758

ENTRY POINT=  0118B810
```

REFERENCES

Barker, S. J., and C. G. Jennings, 1977: "The Effect of Wall Heating on Transition in Water Boundary Layers," AGARD Symposium on Laminar Turbulent Transition, Copenhagen, Denmark, 2-4 May 1977.

Barua, S. N., 1963: "Secondary Flow in Stationary Curved Pipes," *Quart. J. Mech. Appl. Math.*, 16, pp. 61-77.

Dean, W. R., 1927: "Note on the Motion of Fluid in a Curved Pipe," *Phil. Mag.*, 4, pp. 208-223.

Dean, W. R., 1928: "The Stream-line Motion of Fluid in a Curved Pipe," *Phil. Mag.*, 5, pp. 673-695.

Hong, S. W., and A. E. Bergles, 1976: "Theoretical Solutions for Combined Force and Free Convection in Horizontal Tubes with Temperature-Dependent Viscosity," *J. Heat Transfer*, 98, pp. 459-465.

Lighthill, M. J., 1958: *Introduction to Fourier Analysis and Generalized Functions*, Cambridge University Press.

Mori, Y., and K. Futagami, 1967: "Forced Convective Heat Transfer in Uniformly Heated Horizontal Tubes," *Int. J. Heat Mass Transfer*, 10, pp. 1801-1813.

Mori, Y., K. Futagami, S. Tokuda, and M. Nakamura, 1965: "Forced Convective Heat Transfer in Uniformly Heated Horizontal Tubes," *Int. J. Heat Mass Transfer*, 9, pp. 453-463.

Morton, B. R., 1959: "Laminar Convection in Uniformly Heated Horizontal Pipes at Low Rayleigh Numbers," *Quart. J. Mech. Appl. Math.*, 12, pp. 410-420.

Siegwarth, D. P., R. D. Mikesell, T. C. Readal, and T. J. Hanrathy, 1969: "Effect of Secondary Flow on the Temperature Field and Primary Flow in a Heated Horizontal Pipe," *Int. J. Heat Mass Transfer*, 12, pp. 1535-1551.

Singh, M. P., 1974: "Entry Flow in a Curved Pipe," *J. Fluid Mech.*, 65, pp. 517-539.

Taylor, G. I., 1929: "The Criterion for Turbulence in Curved Pipes," *Proc. Roy. Soc.*, A124, p. 243.

Van Dyke, M. D., 1970: "Entry Flow in a Channel," *J. Fluid Mech.*, 44, pp. 813-823.

Wilson, S. D. R., 1971: "Entry Flow in a Channel, Part 2," *J. Fluid Mech.*, 46, pp. 787-799.

Yao, L. S., and S. A. Berger, 1975: "Entry Flow in a Curved Pipe," *J. Fluid Mech.*, 67, pp. 177-196.

Yao, L. S., and I. Catton, 1976a: *Buoyancy Cross-Flow Effects on the Boundary Layer of a Heated Horizontal Cylinder*, The Rand Corporation, R-1907-ARPA. To appear in *J. Heat Transfer*, 1977.

Yao, L. S., and I. Catton, 1976b: *The Buoyancy and Variable Viscosity Effects on a Water Laminar Boundary Layer along a Heated Longitudinal Horizontal Cylinder*, The Rand Corporation, R-1966-ARPA, February 1977.